HIV-1 selectively targets gut-homing CCR6^{+}CD4^{+} T-cells
via mTOR-dependent mechanisms

Delphine Planas[1,2], Yuwei Zhang[1,2], Patricia Monteiro[1,2], Jean-Philippe Goulet[3], Annie Gosselin[1], Nathalie Grandvaux[1,4], Thomas J. Hope[5], Ariberto Fassati[6], Jean-Pierre Routy[7,8], and Petronela Ancuta[1, 2, *]

[1]Centre de recherche du Centre Hospitalier de l'Université de Montréal; [2]Université de Montréal, Faculté de Médecine, Département of microbiologie, infectiologie et immunologie; [3]Caprion, Montréal, Québec, Canada; [4]Université de Montréal, Faculté de Médecine, Département of biochimie et médecine moléculaire, Montréal, Québec, Canada; [5]Department of Cellular and Molecular Biology, Feinberg School of Medicine, Northwestern University, Chicago, IL, USA; [6]University College London, London, UK; [7]Chronic Viral Illness Service and Research Institute, McGill University Health Centre; [8]Division of Hematology, McGill University Health Centre, Montreal, QC, Canada.

Authors' email addresses: delphine.planas@umontreal.ca; zhangyw927@gmail.com; patriciamonteiro2003@yahoo.fr; gouletjp@me.com; annie.gosselin.chum@gmail.com; nathalie.grandvaux@umontreal.ca; thope@northwestern.edu; a.fassati@ucl.ac.uk; jean-pierre.routy@mcgill.ca; and petronela.ancuta@umontreal.ca

*, Corresponding author mailing address: Petronela Ancuta, CHUM-Research Centre, 900 rue Saint-Denis, Tour Viger R, room R09.416, Montreal, Quebec H2X 0A9, Canada; phone: 514-890-8000, extension #35744; FAX: 514 412-7936; e-mail: petronela.ancuta@umontreal.ca

Running title: mTOR regulates HIV in gut-homing Th17 cells

Key words: human, Th17, CCR6, HIV, ATRA, gut-homing, ART

Text count: **11,885 words**
Number of Figures: 11
Number of Supplemental Figures: 8
Number of Supplemental Tables: 6
Number of References: 94

Conflict of interest statement
The authors have declared that no conflict of interest exist

ABSTRACT

Gut-associated lymphoid tissues (GALT) are enriched in CCR6$^+$ Th17-polarized CD4$^+$ T-cells that contribute to HIV-1 persistence during antiretroviral therapy (ART). This raises the need for Th17-targeted immunotherapies. In an effort to identify mechanisms governing HIV-1 permissiveness/persistence in gut-homing Th17 cells, we analyzed the transcriptome of CCR6$^+$ *versus* CCR6$^-$ T-cells exposed to the gut-homing inducer retinoic acid (RA) and performed functional validations in colon biopsies of HIV-infected individuals receiving ART (HIV+ART). Although both CCR6$^+$ and CCR6$^-$ T-cells acquired gut-homing markers upon RA exposure, the modulation of unique sets of genes coincided with preferential HIV-1 replication in RA-treated CCR6$^+$ T-cells. This molecular signature included the up-regulation of HIV-dependency factors acting at entry/post-entry levels, such as CCR5 and PI3K-Akt-mTORC1 signaling pathway. Of note, mTOR expression/phosphorylation was distinctively induced by RA in CCR6$^+$ T-cells. Consistently, mTOR inhibitors counteracted the effect of RA on HIV replication *in vitro* and viral reactivation in CD4$^+$ T-cells from HIV+ART individuals, *via* post-entry mechanisms independent of CCR5. Finally, CCR6$^+$ *versus* CCR6$^-$ T-cells infiltrating the colon of HIV+ART individuals expressed unique molecular signature including higher levels of CCR5, integrin β7, and mTOR phosphorylation. Together, our results identify mTOR as a druggable key regulator of HIV permissiveness in gut-homing CCR6$^+$ T-cells.

INTRODUCTION

Human immunodeficiency virus type 1 (HIV-1) causes the progressive depletion of $CD4^+$ T-cells thus impairing the ability of the immune system to fight pathogens. Although current antiretroviral therapies (ART) efficiently control viral replication and restore CD4 counts, the HIV eradication is not achieved (1-3). Major $CD4^+$ T-cell alterations occur in gut-associated lymphoid tissues (GALT) rapidly upon HIV transmission (4, 5) and these alterations persist despite viral suppressive ART (3, 6), even in patients treated during acute HIV infection (7). The GALT is considered an important site of HIV replication and viral reservoir persistence during ART (8). GALT-infiltrating $CD4^+$ T-cells represent optimal HIV targets likely due to their high expression of CCR5 (4, 5, 8), a major co-receptor for HIV entry (9-11), and integrin α4β7, a gut-homing molecule (12) identified as an HIV-binding molecule (13). Very recently, integrin α4β7 blocking Abs proved efficacy in controlling viral replication upon ART interruption in a SIV infection model (14), indicative that interfering with HIV replication in gut-homing $α4β7^+CD4^+$ T-cells represents a potential curative strategy.

Among GALT-infiltrating $CD4^+$ T-cells, Th17 cells play a beneficial role in maintaining epithelial cell integrity at barrier surfaces *via* the production of effector cytokines under the control of lineage-specific transcription factors (15). Studies by our group and others demonstrated that Th17-polarized $CCR6^+CD4^+$ T-cells are highly permissive to infection (16-18), as a consequence of their expression of HIV dependency factors (HDFs) acting at entry and post-entry levels (19, 20), combined with the lack of HIV restriction mechanisms (21-23). Most recently, $CD4^+$ T-cells expressing the Th17

markers CCR6/RORγt were identified as the first targets of SIV during vaginal transmission (24); also, the detrimental role of viral permissive CCR6$^+$ T-cell infiltration into the gut was documented (25). The depletion of Th17 cells from the GALT upon HIV infection persists despite viral-suppressive ART (26-28), even when ART is intensified with integrase and CCR5 inhibitors (29). Other promising strategies tested for mucosal Th17 restoration include an ideal ART initiation at very early stages of infection (Fiebig I/II but not III) (7), the use of probiotics, and IL-21 supplementation (30-32). The non-restoration of GALT Th17 cells leads to significant damages of the intestinal barrier thus allowing the microbial translocation, a cause for chronic immune activation and occurrence of non-AIDS co-morbidities during ART (3, 6, 33). Despite their dramatic depletion, long-lived Th17 cells contribute to HIV reservoir persistence during ART (34, 35). Consistently, our group identified a subset of CCR6$^+$CCR4$^-$CXCR3$^-$ Th17 cells predominant in blood and lymph nodes and carrying replication-competent HIV reservoirs (36) and further demonstrated preferential HIV-DNA persistence in colon infiltrating CCR6$^+$CD4$^+$ T-cells during ART (37). These advances orient our search for immunotherapeutic strategies to limit HIV infection/persistence in mucosal Th17 cells in the ART era.

The homing of CCR6$^+$ Th17 cells into the GALT is mediated *via* the CCR6/CCL20 axis (28, 38), as well as the adhesion molecule integrin α4β7 (12) and chemokine receptor CCR9 (39). The imprinting for gut-homing is induced by *all-trans* retinoic acid (ATRA) (40), a vitamin A metabolite produced by GALT dendritic cells (41). Our previous studies demonstrated that ATRA increases HIV-1 permissiveness

preferentially in CCR6$^+$ compared to CCR6$^-$ T-cells (42). This effect coincided with the preferential ability of ATRA to up-regulate the expression of the HIV co-receptor CCR5 on CCR6$^+$ T-cells, indicative of a most efficient HIV entry. Nevertheless, exposure to single-round VSV-G-pseudotyped HIV entering cells by endocytosis provided evidence that ATRA also promotes HIV replication in gut-homing CCR6$^+$ T-cells *via* post-entry mechanisms (42). These findings led to the current hypothesis that CCR6 is a marker for Th17-polarized CD4$^+$ T-cells transcriptionally programmed to become HIV targets in the gut, where ATRA promotes the expression of unidentified HIV permissiveness factors, which may be manipulated to protect gut-homing Th17 cells from HIV.

In our search for new druggable molecular targets to prevent HIV replication/persistence in gut-homing Th17 cells, herein we performed a genome-wide transcriptional profiling to identify HDFs modulated by ATRA in memory CCR6$^+$ T-cells. Together, our studies *i)* provide an in-depth characterization of molecular mechanisms contributing to HIV replication/persistence in ATRA-exposed CCR6$^+$ Th17 cells; *ii)* identified mTOR as a druggable target modulated by ATRA in these cells; and *iii)* support the beneficial use of mTOR inhibitors in clinics to preserve mucosal Th17 cells from HIV infection/persistence during ART.

RESULTS

Transmitted/founder (T/F) HIV preferentially infects retinoic-acid treated CCR6$^+$CD4$^+$ T-cells. We previously reported that *all-trans* retinoic acid (ATRA) mediated-imprinting for gut-homing increases replication of the laboratory-adapted R5 NL4.3BaL HIV preferentially in CCR6$^+$ *versus* CCR6$^-$ T-cells (42). T/F HIV strains are isolated early upon seroconversion and are unique in their virulence/sensitivity to antiviral mechanisms (43). To determine whether T/F HIV also target gut-homing CCR6$^+$ T-cells for preferential replication, FACS-sorted memory CCR6$^+$ and CCR6$^-$ T-cells stimulated *via* CD3/CD28 in the presence/absence of ATRA were exposed in parallel to T/F THRO (44) and NL4.3BaL HIV (Figure 1A). The relative frequency of CCR6$^+$ and CCR6$^-$ T-cells in peripheral blood mononuclear cells (PBMCs) before sort is depicted in Figure 1B-C. The dose of ATRA used (10 nM) (42) is consistent with physiological plasma levels (40) and had no influence on cell viability (data not shown). ATRA robustly increases replication of both NL4.3BaL and T/F THRO HIV in CCR6$^+$ T-cells, while the effects on CCR6$^-$ T-cells were only minor, as reflected by the quantification of early (RU5), late (Gag), and integrated (Alu/HIV) HIV reverse transcripts (Figure 1 D-E). Thus, T/F similar to NL4.3BaL HIV also target ATRA-treated CCR6$^+$ T-cells for preferential replication, suggesting a critical role played by gut-homing CCR6$^+$ T-cells during the early steps of mucosal HIV transmission.

CCR6$^+$ *versus* CCR6$^-$ T-cells exhibit higher proliferation, TNF-α production, and NF-κB DNA-binding activity in the presence/absence of ATRA. In search of post-entry permissiveness mechanisms, we first investigated whether ATRA modulated

proliferation and IL-2 production. In the absence of ATRA, CCR6$^+$ compared to CCR6$^-$ T-cells exhibited higher proliferation upon TCR triggering but a markedly lower production of IL-2 (Suppl. Figure 1A-C), consistent with previous studies (16), likely as a consequence of RORγt-mediated IL-2 inhibition (45). ATRA further decreased IL-2 production in CCR6$^+$ T-cells but had no significant effect on cell proliferation (Suppl. Figure 1A-C). Levels of CD25 (IL-2Rα) were similarly high on CCR6$^+$ and CCR6$^-$ T-cells exposed or not to ATRA (Suppl. Figure 1D-G), indicative that differences in IL-2 production are not related to IL-2 auto-consumption. Thus, increased HIV replication in CCR6$^+$ T-cells upon exposure to ATRA cannot be explained by enhanced cell proliferation and/or IL-2 production.

HIV permissiveness in CCR6$^+$Th17 *versus* CCR6$^-$Th1 cells is associated with higher NF-κB nuclear translocation (20). The pro-inflammatory cytokine TNF-α enhances HIV replication, in part by triggering the NF-κB pathway (46). This prompted us to investigate differences in TNF-α production and NF-κB-p65 activity. Upon TCR triggering, CCR6$^+$ *versus* CCR6$^-$ T-cells produced significantly higher levels of TNF-α in the absence of ATRA; although ATRA slightly decreased TNF-α production in CCR6$^+$ T-cells, levels remained significantly higher in ATRA-treated CCR6$^+$ *versus* CCR6$^-$ T-cells (Suppl. Figure 2A). The NF-κB-p65 DNA-binding activity was higher in CCR6$^+$ *versus* CCR6$^-$ T-cell nuclei when cells were cultured in the presence/absence of ATRA; exposure to ATRA slightly decreased NF-κB-p65 DNA-binding activity in CCR6$^+$ T-cells (Suppl. Figure 2B), consistent with previous reports (47). Nevertheless, NF-κB-p65 DNA-binding activity remained significantly higher in ATRA-treated CCR6$^+$ *versus*

7

CCR6$^-$ T-cells (Suppl. Figure 2B). Together these results demonstrate that TNF-α production and NF-κB-p65 nuclear translocation/DNA-binding activity are significantly higher in memory CCR6$^+$ *versus* CCR6$^-$ T-cells upon TCR triggering, but ATRA has no positive impact on these differences.

ATRA promotes a unique transcriptional program associated with HIV permissiveness in CCR6$^+$ T-cells. To gain insights into mechanisms underlying the differential effects of ATRA on CCR6$^+$ *versus* CCR6$^-$ T-cells, their ability to integrate ATRA-mediated signals was investigated. CCR6$^+$ and CCR6$^-$ T-cells expressed similar levels of RA receptor alpha (RARα) mRNA *ex vivo* (Figure 2A) and ATRA up-regulated the expression of RA-inducible gene I (RIG-I)/Retinoic acid receptor responder protein 3 (RARRES3), a direct target of RA (48), in both cell subsets (Figure 2B). We hypothesized that CCR6$^+$ and CCR6$^-$ T-cell subsets respond to ATRA in distinct fashions, with the expression of HIV dependency factors (HDFs) being promoted preferentially in CCR6$^+$ T-cells. To test this hypothesis, a genome-wide transcriptional profiling was performed in CCR6$^+$ and CCR6$^-$ T-cells stimulated *via* the TCR in the presence/absence of ATRA for four days; this time point coincided with the time of HIV exposure in Figure 1.

Differentially expressed genes were identified based on p-values (p) or adjusted p-values (adj. p) and fold change (FC) of gene expression. Results in Figure 2C and Suppl. Tables 1-4 illustrate transcriptional differences between CCR6$^+$ and CCR6$^-$ T-cells upon TCR triggering in the presence/absence of ATRA. In the absence of ATRA, up-regulated

transcripts (n=348; adj. p-values<0.05, FC cut-off 1.3) in CCR6$^+$ *versus* CCR6$^-$ T-cells included Th17 markers such as CCL20, IL-22, IL-17F, CTSH, KLRB1/CD161, IL-8, RORA, CSF2/GM-CSF, IL-26, RORC, CCR6, SGK1, PPARG, IL-23R, ARNTL, and PTPN13 (Suppl. Table 1). Transcripts up-regulated by ATRA in CCR6$^+$ T-cells (n=95; adj. p-values<0.05, FC cut-off 1.3) included RARRES3, CD38, DHRS3, UBD, LGMN, EVI5, LZTFL1, NAPSA, GBP4, HIC1, CCR9, CCR2, CXCR6, and ITGB7 (Suppl. Table 2). Transcripts up-regulated by ATRA in CCR6$^-$ T-cells (n=119; adj. p-values<0.05, FC cut-off 1.3) included NAPSA, CD38, EVI5, SAMD9, GALR2, DHRS3, ANKRD37, PTGER2, SLC26A4, and RARRES3, ARG2, APOBEC3B, RIPK2, and NFIL3 (Suppl. Table 3). The analysis of the n=319 transcripts over expressed in ATRA-treated CCR6$^+$ *versus* CCR6$^-$ T-cells revealed the preservation of a Th17 signature (*e.g.,* CCL20, IL-17F, CTSH, IL-22, KLRB1, CSF2, ANTXR2, GPR56, CXCR6, KLF2, RORC, RORA, S100A4, CCR6, MAP3K4, CD96, IL-26, FURIN, ABCB1, ARNTL, and PTPN13) (Suppl. Table 4). Finally, in the presence/absence of ATRA, CCR6$^+$ *versus* CCR6$^-$ T-cells show superior expression of the Th17 markers RORC, ARNTL, and CCR6, and inferior expression of the RORC nuclear repressor NFIL3 (49) (Suppl. Figure 3). Together these results demonstrate that CCR6$^+$ and CCR6$^-$ T-cells respond to ATRA in a unique transcriptional fashion and that ATRA exposure does not modify the Th17-polarisation profile of CCR6$^+$ T-cells.

An extended intelligent search within top modulated transcripts revealed that ATRA induced expression of gut-homing markers integrin α4, integrin β7 and CCR9 (12) in both CCR6$^+$ and CCR6$^-$ T-cells. Of note, CXCR6, a minor HIV co-receptor (50, 51), was

significantly up-regulated by ATRA in CCR6$^+$ but not CCR6$^-$ T-cells (Suppl. Tables 2-4; Suppl. Figure 3). FACS analysis validated the microarray results for integrin β7 and CXCR6 expression (Suppl. Figure 4A-C). Although CCR5 transcripts were not differentially expressed in microarrays (data not shown), we confirm (42) that ATRA significantly up-regulates CCR5 preferentially on CCR6$^+$ T-cells (Suppl. Figure 4A and D). This coincided with the up-regulation of KLF2 (Suppl. Figure 3), a positive regulator of CCR5 transcription (52). The down-regulation of CCR5 ligands CCL3 and CCL3L1 by ATRA was mainly observed in CCR6$^+$ T-cells, indicative of a more efficient CCR5-mediated HIV entry (53). Although the T-cell activation marker CD38 was similarly up-regulated by ATRA in both subsets (Suppl. Figure 3), transcripts for MAP3K4, a Th17-specific kinase (54) we previously identified as a HDF (20), were expressed at superior levels and up-regulated by ATRA in CCR6$^+$ *versus* CCR6$^-$ T-cells (Suppl. Figure 3). Moreover, the transcripts for PPARγ, a transcriptional repressor of RORγt (55) and Th17-intrinsec negative regulator of HIV replication (19), was down-regulated by ATRA specifically in CCR6$^+$ T-cells (Suppl. Figure 3). Furthermore, CCR6$^+$ *versus* CCR6$^-$ T-cells stimulated *via* the TCR in the presence/absence of ATRA expressed decreased levels of interferon (IFN) stimulated genes, such as IFITM1, 2, and 3, and IRF8 (Suppl. Tables 1-4), consistent with the low Th17 ability to respond to IFN (23). Finally, although differences in the expression of SAMHD1, a key IFN-induced HIV restriction factor (22, 56, 57), were not observed in the microarrays, in the presence/absence of ATRA, levels of SAMHD1 mRNA measured by RT-PCR were significantly lower in CCR6$^+$ *versus* CCR6$^-$ T-cells (Suppl. Figure 5). This stresses the existence of false negatives in high-throughput transcriptional screenings. Together, these findings reveal

multiple HDFs acting at entry and post-entry levels to facilitate HIV replication in ATRA-treated CCR6$^+$ T-cells, as well as a state of antiviral immunity acting at different levels in CCR6$^-$ T-cells.

Among probe sets differentially modulated by ATRA in CCR6$^+$ and CCR6$^-$ T-cells, (p-value<0.05), only 466 transcripts were shared, while 1,285 and 1,538 transcripts were unique to CCR6$^+$ and CCR6$^-$ T-cells, respectively (Figure 2D). A meta-analysis using the NCBI HIV-1 interactions data-base allowed the identification of human genes previously described to enhance HIV-1 protein expression that were differentially regulated by ATRA in CCR6$^+$ *versus* CCR6$^-$ T-cells (Suppl. Figure 6). Among those transcripts, LGALS3, ADAM15, TRIM8, IL-1α, FOXO3, and ARNTL were up-regulated by ATRA in CCR6$^+$ *versus* CCR6$^-$ T-cells (Suppl. Figure 3 and 6).

Finally, Gene Set Variation Analysis (GSVA) identified pathways modulated by ATRA in CCR6$^+$ T-cells, including the Akt and PI3K signaling pathways (Figure 3), critical for the Th17 polarization (58-60). A custom pathway was created using the genes from BIOCARTA_AKT_PATHWAY and PID_PI3K_PLC_TRK_PATHWAY, genes that were differentially modulated by ATRA in CCR6$^+$ T-cells (Figure 4A). Of note, the mammalian target of rapamycin (mTOR) appeared up-regulated by ATRA in CCR6$^+$ T-cells in this gene interaction network representation (Figure 4A). Ingenuity Pathway Analysis (IPA) was further used to illustrate genes associated with the mTORC1 pathway and regulated by ATRA in CCR6$^+$ T-cells (Figure 4B).

Together, this genome-wide transcriptional analysis reveals unique molecular signatures associated with HIV permissiveness in Th17-polarized CCR6^{+} T-cells upon exposure to ATRA and point to a critical role played by mTOR in this process.

ATRA induces mTOR expression and phosphorylation selectively in CCR6^{+} T-cells.
To explore the potential contribution of mTOR to HIV permissiveness in ATRA-treated CCR6^{+} T-cells, the expression of total and phosphorylated mTOR was first investigated by western blotting in sorted CCR6^{+} and CCR6^{-} T-cells stimulated *via* the TCR in the presence/absence of ATRA. Levels of total/phosphorylated mTOR were low to undetectable in TCR-activated CCR6^{+} T-cells but significantly increased by ATRA treatment. In contrast, TCR-activated CCR6^{-} T-cells expressed high levels of total/phosphorylated mTOR and ATRA did not modify this expression (Figure 5A-B). The molecular weight of the main mTOR band was 80 kDa, which corresponds to the β isoform of mTOR typically expressed in T-cells (61). To further validate these results, we performed semi-quantitative RT-PCR and visualized on gel the expression of mTOR mRNA corresponding to isoform β (2,118 Kb), using established primers (61). Levels of mTOR isoform β mRNA were significantly higher in CCR6^{+} T-cells upon exposure to ATRA (Suppl. Figure 7). The findings that mTOR mRNA expression and mTOR phosphorylation are induced by ATRA preferentially in CCR6^{+} T-cells point to the existence of mTOR-dependent HIV permissiveness mechanisms in gut-homing CCR6^{+} T-cells.

mTORC1/2 inhibitors counteract the effect of ATRA on HIV replication. To determine the functional role of ATRA-mediated mTOR activity, two commercially available mTOR inhibitors were tested for their ability to counteract the effect of ATRA on HIV permissiveness: rapamycin, an inhibitor of mTORC1, and INK128, an inhibitor of mTORC1/2 (62). Memory CD4$^+$ T-cells were stimulated *via* the TCR and further exposed to HIV in the presence/absence of ATRA, rapamycin or INK128 (Figure 6A). Rapamycin and INK128 significantly reduced levels of early/late reverse transcripts and integrated HIV-DNA in ATRA-treated T-cells from five different donors, with INK128 having the most robust inhibitory effects, especially when added before and after infection (Figure 6B-D). Similarly, rapamycin and most significantly INK128 had a robust inhibitory effect on HIV replication measured by HIV-p24 ELISA at days 3, 6 and 9 post-infection (Figure 6E). Of note, the treatment with mTOR inhibitors in combination with ATRA significantly reduced the ability of cells to produce IL-17A but did not alter IFN-γ production, cell viability and proliferation (Suppl. Figure 8A-D). Similar experiments were further performed with FACS-sorted memory CCR6$^+$/CCR6$^-$ T-cells. INK128 significantly reduced HIV integration/replication in ATRA-treated CCR6$^+$ T-cells. Although levels of HIV integration/replication were lower in CCR6$^-$ compared to CCR6$^+$ T-cells, INK128 similarly acted on CCR6$^-$ T-cells (Figure 7A-B), consistent with the mTOR expression in these cells (Figure 5; Suppl. Figure 7). Together, these results support the role of ATRA-induced mTOR signaling pathway as a positive regulator of HIV permissiveness in gut-homing CCR6$^+$ T-cells.

mTORC1/2 inhibitors limit HIV replication at post-entry level in ATRA-treated T-cells. Studies in humanized mice demonstrated the ability of rapamycin and INK128 to inhibit HIV replication *via* the regulation of CCR5 expression (62). To investigate this possibility, we tested the effects of rapamycin and INK128 on CCR5 expression in memory CD4$^+$ T-cells stimulated *via* TCR in the presence/absence of ATRA. Although rapamycin and INK128 significantly reduced CCR5 expression in the absence of ATRA, no significant changes were observed in the presence of ATRA (Figure 8A-B). Similarly, rapamycin and INK128 had no significant effects on the expression of integrin β7 (Figure 8C-D), a gut-homing molecule induced by ATRA (12) that was also identified as an HIV-gp120 binding molecule (13). To further distinguish between HIV entry and post-entry mTOR-mediated mechanisms in the context of ATRA, we performed a single-round infection using replication-defective VSV-G-pseudotyped HIV and tested the effects of rapamycin or INK128 on HIV reverse transcription and integration. Both rapamycin and INK128 induced a partial decrease in levels of early (59±3 and 65±7% inhibition) and late (88±2 and 90±5% inhibition) HIV reverse transcript and an almost complete abrogation of HIV-DNA integration (98±0.1 and 99±0.1% inhibition, n=3) (Figure 8E-G). Together these results demonstrate that mTORC1/2 inhibitors limit HIV replication in gut-homing CCR6$^+$CD4$^+$ T-cells *via* post-entry mechanisms, during reverse transcription and prior to integration, without impact on CCR5- and/or integrin β7-mediated viral entry or cell homing into the gut.

ATRA promotes HIV reactivation in CD4$^+$ T-cells of ART-treated individuals in an mTOR-dependent manner. In a very recent study, we demonstrated that ATRA

facilitates HIV reactivation from latency in CCR6$^+$CD4$^+$ T-cells from ART-treated individuals (37). To determine whether HIV reservoir reactivation was dependent on mTOR activity, an optimized viral outgrowth assay (VOA) was performed in the presence/absence of ATRA and mTORC1/2 inhibitor INK128 (Figure 9A). Consistent with previous findings (37), ATRA significantly improved the efficacy of HIV reactivation in memory CD4$^+$ T-cells isolated from ART-treated individuals (Suppl. Table 5), as measured by intracellular HIV-p24 staining (Figure 9B-C) and soluble HIV-p24 in cell-culture supernatants at day 12 post-reactivation (Figure 9D). Of particular importance, INK128 inhibited HIV reactivation mediated by TCR triggering in the presence of ATRA (Figure 9B-D). Further, we tested the effects of INK128 on HIV reservoir reactivation in memory CCR6$^+$ and CCR6$^-$ T-cells isolated by FACS from ART-treated individuals (Suppl. Table 5). In the absence of ATRA, HIV reactivation was observed in CCR6$^+$ but not CCR6$^-$ T-cells in 1/3 donors (ART #3), while in the presence of ATRA HIV reactivation occurred in 3/3 donors preferentially (ART #3) or only (ART#4 and ART #6) in CCR6$^+$ T-cells. Of particular importance, INK128 dramatically reduced HIV reactivation in ATRA-treated CCR6$^+$ T-cells, as measured by intracellular HIV-p24 expression (Figure 9E-F) and soluble HIV-p24 production in cell-culture supernatants at day 12 post-reactivation (data not shown). Together, these results reveal mTOR as a key player in ATRA-mediated HIV reactivation in CCR6$^+$ T-cells of ART-treated individuals.

Colon-infiltrating CCR6$^+$CD4$^+$ T-cells express high levels of CCR5, integrin β7, and phosphorylated mTOR. The GALT is enriched in DCs metabolizing vitamin A into

ATRA (41). We further explored whether the molecular "*signature*" induced by ATRA *in vitro* including the up-regulation of CCR5, integrin β7 and mTOR phosphorylation on CCR6^{+} T-cells can be observed as well in the GALT. To test this possibility, we had access to matched blood and sigmoid biopsies from n=10 HIV-infected individuals receiving ART (Suppl. Table 5; COL #1-10). Memory CD4^{+} T-cells were identified using the gating strategy depicted in Figure 10A and further analyzed for the expression of CCR5, integrin β7, and phosphorylated mTOR in CCR6^{+} *versus* CCR6^{-} T-cells. The expression of CCR5 and integrin β7 was higher on cells from the colon *versus* the blood; with colon-infiltrating CCR6^{+} *versus* CCR6^{-} T-cells expressing significantly higher levels of CCR5 and integrin β7 (Figure 10B-E). Similarly, mTOR phosphorylation was mainly observed in the colon, with colon-infiltrating CCR6^{+} *versus* CCR6^{-} T-cells expressing the highest levels of phosphorylated mTOR in all individuals tested (Figure 10F-G). Thus, the activation of the mTOR pathway occurs almost exclusively in colon-infiltrating CCR6^{+} T-cells and coincides with the highest levels of CCR5 and integrin β7 expression. These results provide a molecular explanation for the preferential HIV replication in colon CCR6^{+} T-cells and point to mTOR as a new antiviral drug target in these cells (Figure 11).

Discussion

The role of *all-trans* retinoic acid (ATRA) in regulating tolerance and immunity *via* the modulation of regulatory and effector functions of CD4$^+$ T-cells, respectively, is well-established (41). Our current results support the idea that in the intestinal environment HIV takes advantage of ATRA-mediated signaling pathways for replication/persistence in CCR6$^+$CD4$^+$ T-cells. Briefly, we *i)* identified mTOR as a major regulator of HIV permissiveness in CCR6$^+$CD4$^+$ T-cells with gut-homing tropism mimicked *in vitro* by exposure to ATRA; *ii)* demonstrated the ability of mTOR inhibitors to counteract the effects of ATRA on HIV replication *in vitro* and viral reservoir reactivation in T-cells from ART-treated individuals; and *iii)* revealed that CCR6$^+$CD4$^+$ T-cells infiltrating the colon of HIV-infected individuals on ART express a unique signature comprising high levels of CCR5, integrin β7, and phosphorylated mTOR, signature likely reflecting exposure to ATRA *in vivo* (Figure 11). Considering the strategic location of Th17 cells at portal sites of HIV/SIV entry (6, 24, 27, 28, 63), as well as their important role in maintaining mucosal immunity homeostasis in the context of a complex microbiota (6, 64, 65), our results point to the potential beneficial use of mTOR inhibitors in preventing HIV infection/persistence in gut-homing Th17 cells.

In this manuscript, we used the Illumina bead array technology to unveil post-entry HIV regulatory mechanisms modulated by ATRA in CCR6$^+$ *versus* CCR6$^-$ T-cells. Among genes commonly modulated by ATRA in CCR6$^+$ and CCR6$^-$ T-cells, the RA-inducible gene-I (RIG-I) is essential for sensing of viral nucleic acids and promoting antiviral immunity (66). HIV is known to subvert RIG-I-mediated antiviral mechanisms (67); this

may explain robust HIV replication in RIG-I-expressing ATRA-treated CCR6$^+$ T-cells. Of particular importance, Li *et al*. recently demonstrated that acitretin, a RA derivative, increases HIV transcription in CD4$^+$ T-cells from ART-treated HIV-infected individuals and enhances RIG-I signaling thus leading to an antiviral response and the apoptosis of infected cells (68). Similarly, in a previous report (37) and in this manuscript, we demonstrated that ATRA significantly increases HIV reactivation in a viral outgrowth assay (VOA) without significant changes observed in T-cell survival/proliferation. Differences between our results and those published by Li *et al.* (68), may be explained by differences in the experimental design. Nevertheless, these findings commonly support the fact that ATRA promotes HIV reservoir reactivation.

A meta-analysis using the NCBI HIV interaction database revealed HDFs preferentially expressed by ATRA-exposed CCR6$^+$ T-cells. These HDFs include LGALS3, promoting HIV-1 budding *via* association with Alix and Gag p6 (69); ADAM15, involved in the nuclear import of the HIV-1 pre-integration complex (70); TRIM8, a regulator of NF-κB and STAT3-dependent signaling cascades (20, 71); and ARNTL (72), a component of the circadian clock machinery and regulator of Th17 development (49). All these HDFs contribute to robust HIV replication in gut-homing CCR6$^+$ T-cells.

Gene Set Variation Analysis (GSVA) of transcripts uniquely modulated by ATRA in CCR6$^+$ T-cells identified unique pathways, including Akt and PI3K. The network representation of Akt/PI3K pathways, previously linked to Th17 lineage polarization (58-60) and reported to be up-regulated in human lamina propria T-cells (73), pointed to

the up-regulation of mTOR, a metabolic sensor involved in the regulation of numerous cellular functions *via* the formation of two different signaling complexes, mTORC1 and mTORC2 (74-77). Considering the documented role of mTOR-mediated processes in the positive regulation of HIV replication (62, 78), we proceeded to the validation of mTOR expression at protein and mRNA levels, as well as functional validations, in cells from the blood and/or colon of HIV-infected individuals receiving ART and uninfected study participants.

The regulation of HIV permissiveness *via* mTOR-dependent mechanisms was demonstrated by the use of mTORC1 (rapamycin) and/or mTORC1/2 (INK128) inhibitors, that counteracted the effects of ATRA on HIV replication in CCR6$^+$ T-cells *in vitro* and inhibited HIV reservoir reactivation in an ATRA-based VOA performed with CCR6$^+$ T-cells from ART-treated individuals. Nevertheless, mTOR expression/phosphorylation is not always associated with HIV permissiveness. Indeed, CCR6$^-$ T-cells are relatively resistant to HIV despite high levels of mTOR expression, likely due to the existence of HIV restriction mechanisms acting at different levels including entry (low/undetectable CCR5 expression), reverse transcription (high SAMHD1 expression), and/or transcription (limited TNF-α production and NF-κB activity). Thus, mTOR favors HIV replication/reactivation only within the unique transcriptional context of ATRA-exposed CCR6$^+$ T-cells.

Evidence exists in the literature that mTOR regulates HIV replication *via* multiple mechanisms (78, 79). One possible mechanism is *via* the regulation of CCR5 expression

(62). However, CCR5 expression on ATRA-treated T-cells was not affected by mTOR inhibitors. This suggests that ATRA induces CCR5 expression *via* mTOR-independent mechanisms and that mTOR regulation of HIV permissiveness in gut-homing CD4$^+$ T-cells likely occurs at post-entry levels. Consistent with the evidence that mTOR regulates nucleotide biosynthesis essential for transcription (76, 80, 81), mTOR inhibitors may limit HIV reverse transcription by reducing the pool of nucleotides. Indeed, our single-round infection using VSV-G-pseudotyped HIV revealed restriction mechanisms acting during reverse transcription and prior to integration. Moreover, mTOR is a well-established regulator of autophagy (79, 82), a process that may be involved in the degradation of the incoming HIV upon fusion/uncoating (83, 84). By promoting the mTOR activity, ATRA may impair the autophagy process in CCR5$^+$CCR6$^+$ T-cells at mucosal sites. Furthermore, considering the fact that ATRA-treated CCR6$^+$ T-cells maintain their Th17 features (42) and that mTORC1 *via* the induction of the kinase S6K2 is involved in the nuclear translocation of RORC (60, 85), one other possibility is that mTOR inhibitors interfere with the RORC-mediated transcriptional program in Th17 cells, which is favorable to HIV replication (20). Consistent with this hypothesis, we demonstrated that decreased HIV replication in the presence of rapamycin and INK128 coincided with a significant reduction in IL-17A production by ATRA-treated CD4$^+$ T-cells.

Of particular importance, we found that CCR6$^+$ but not CCR6$^-$ T-cells infiltrating the colon of HIV-infected individuals receiving ART express a unique molecular signature including superior levels of CCR5, integrin β7 and phosphorylated mTOR expression,

likely as a consequence of ATRA exposure in the intestinal environment (12, 41). In line with our recent report that HIV-DNA persists in colon-infiltrating CCR6^{+} T-cells during ART (37), it remains to be determined whether mTOR expression identifies a fraction of CCR6^{+} T-cells enriched in HIV-DNA and whether mTOR activation contributes to residual HIV replication in colon-infiltrating CCR6^{+} T-cells during ART.

While this manuscript was in preparation for submission, Besnard *et al.* reported the results of a shRNA screen that revealed mTOR as a regulator of HIV latency (86) via mechanisms involving CDK9 and NF-κB activation that controls Tat-dependent HIV transcription (86). Also, Martin *et al.* reported on the potential beneficial use of rapamycin in the context of HIV "*shock-an-kill*" strategies (87). These two reports (86, 87) further support the conclusions of our current study revealing the key role played by mTOR in regulating multiple post-entry and post-integration HIV replication steps in gut-homing Th17-polarized CCR6^{+} T-cells.

In conclusion, our findings point to CCR6 as a "zip code" molecule expressed on the surface of CD4^{+} T-cells transcriptionally programmed to become HIV targets upon recruitment into the intestine and provide the first detailed molecular explanation for preferential HIV/SIV replication and persistence in gut-homing CCR6^{+}CD4^{+} T-cells (24, 25, 37, 42). Most significantly, we reveal the role of the mTOR pathway in regulating effector functions as well as HIV permissiveness in gut-homing CCR6^{+} Th17 cells at multiple post-entry levels. Additionally, we demonstrate the ability of mTOR inhibitors to counteract the effects of ATRA on HIV replication/reactivation in CCR6^{+} T-cells. Our

findings raise new questions on the potential beneficial effects of mTOR inhibitors in decreasing HIV reservoirs and restoring the Th17-mediated immunity at the intestinal level during ART. This knowledge will open the path for new studies toward the implementation of new therapeutic strategies aimed at HIV functional cure.

EXPERIMENTAL PROCEDURES

Study subjects

Study subjects were recruited at the Montreal Chest Institute, McGill University Health Centre, and CHUM-Hôpital Saint-Luc (Montreal, Quebec). PBMCs were collected by leukapheresis (88) and cryopreserved until use. Sigmoid biopsies (≈32 biopsies/donor) were collected from HIV-infected individuals receiving antiretroviral therapy (ART) (Suppl. Table 5) during colonoscopy and processed using Liberase DL (Roche Diagnostics), as previously described (37, 89, 90). Matched peripheral blood (20 ml/donor) was collected the same day from biopsy donors.

Flow cytometry staining

Surface staining was performed with fluorochrome-conjugated Abs (Suppl. Table 6), as previously described (16). Cells extracted from sigmoid biopsies and matched PBMCs were stained on the surface with a cocktail of CD3-Alexa700, CD4-PE-Cy7, CD45RA-APC-eF780, CCR5-FITC, integrin β7-FITC, and CCR6-PE Abs, as well as non-T cell lineage Abs: CD326-BV650, CD8-PerCP-Cy5.5, CD19-PerCP-Cy5.5, CD66b-PerCP-Cy5.5 (37). Intracellular staining was subsequently performed with phosphorylated-mTOR (S2448)-eFluor-450 Abs (eBiosciences). The viability dye LIVE/DEAD® Fixable Aqua Dead Cell Stain Kit (Invitrogen) was used to exclude dead cells. Cells were analyzed using a LSRII cytometer, Diva version 6 (BD Biosciences, San Jose, CA), and FlowJo version 10.0.6 (Tree Star, Inc). Flow cytometry gates were defined using the *fluorescence minus one* (FMO) strategy (16, 91).

Magnetic (MACS) and fluorescence activated cell sorting (FACS)

Total or memory CD4$^+$ T-cells were enriched from PBMCs by negative selection using magnetic beads (MACS, Miltenyi), with a purity >95%, as previously described (42). Cells were then stained with CD45RA-APC-Cy7 and CCR6-PE Abs and a cocktail of FITC-conjugated Abs to exclude CD8$^+$ T-cells (CD8), NK (CD56), and B cells (CD19). The sorting gates were set on FITCneg memory (CD45RAneg) CCR6$^+$/CCR6$^-$ T-cells that were subsequently sorted by flow cytometry (BDAria III), with dead cells being excluded. Post-sort quality control analysis demonstrated >97% CCR6$^+$/CCR6$^-$ T-cell purity, as previously reported (42).

HIV-1 infection *in vitro*

The following HIV-1 molecular clones were used in this study: *(i)* replication-competent CCR5-using (R5) NL4.3BAL; *(ii)* single-round VSVG-HIV-GFP, an *env*-deficient NL4.3 provirus pseudotyped with the VSV-G envelope and encoding for *gfp* in place of *nef* (42, 92); and *(iii)* replication-competent Transmitted/Founder (T/F) THRO. The full-length T/F THRO HIV-1 Infectious Molecular Clone (Cat #11919) was obtained from Dr. John Kappes through the NIH AIDS Reagent Program, Division of AIDS, NIAID, NIH (44). HIV stocks were produced, titrated, and used to infect cells (25-50 ng HIV-p24/10^6 cells), as previously described (16, 19, 20, 36, 42).

Quantification of integrated and Gag HIV-DNA

Levels of integrated and Gag HIV-DNA were quantified in cell lysates by ultrasensitive nested real-time PCR (10^5 cells/test in triplicates; detection limit, 3 HIV-DNA copies), as previously described (16, 19, 20, 36, 37, 42, 93).

Quantification of early HIV reverse transcripts

Early HIV reverse transcripts (RU5) were quantified using a SYBR™ Green master mix (Qiagen). The external primers were: forward AA55 5'-CGTCTAGAGATTTTCCACAC-3' and reverse M667 5'-CTAACTAGGGAACCCACTG-3'. The internal primers were: forward SK29 5'-ACTAGGGAACCCACTGCT-3' and reverse SK30 5'-GGTCTGAGGGATCTCTAG-3' (94). The HIV and CD3 DNA were amplified together in the first PCR and separately during the second PCR (LightCycler; Roche). The first PCR products (diluted 1/10) were used as template for the second PCR: 5 min at 94°C, 35 cycles of 1 min at 94°C, 1 min at 50°C, and 30 sec at 72°C; and final elongation of 15 min at 72°C. The ACH2 cells carrying one copy of integrated HIV DNA per cell (NIH AIDS reagent program) were used as a standard curve, as previously described (16, 19, 20, 36, 37, 42, 93).

Genome-wide transcriptional profiling

Genome-wide transcriptional profiling was performed in collaboration with Génome Québec (Montreal, Quebec, Canada) using the Illumina bead array technology, as previously described (20). Briefly, total RNA was isolated using the RNeasy kit (Qiagen) and quantified using the Pearl nanophotometer (Implen, Germany). The RNA quality was

determined using the Agilent 2100 Bioanalyzer chip. High quality RNA was reverse transcribed and hybridized on the Illumina HumanHT-12 v4 Expression BeadChip providing coverage for more than 47,000 transcripts and known spliced variants across the human transcriptome. The expression of differentially expressed genes was analyzed as previously described (19, 20, 36). The entire microarray dataset and technical information requested by Minimum Information About a Microarray Experiment (MIAME) are available at the Gene Expression Omnibus (GEO) database under accession number GSE93660. Differentially expressed genes (cut-off 1.3-fold; $p < 0.05$) were classified through Gene Ontology using the NetAffx web-based application (Affymetrix), while differentially expressed pathways were identified using *Ingenuity Pathway Analysis* (IPA) and *Gene Set Variation Analysis* (GSVA). Corresponding heat maps for biological function categories were generated using programming language R (19, 20, 36).

Real-time RT-PCR

One step SYBR Green real-time RT-PCR (Qiagen) was carried out in a LightCycler 480 II (Roche) according to manufacturer's recommendations, as we previously reported (16, 19, 20, 36, 42). Briefly, a standard curve was prepared with cDNA obtained upon reverse transcription of total RNA using specific QuantiTect Primers (Qiagen). The expression of each gene was normalized to the internal control 28S rRNA (forward 5′-CGAGATTCCTGTCCCCACTA-3′; reverse 5′-GGGGCCACCTCCTTATTCTA-3, IDT). Melting curve analysis performed after real-time amplification revealed the uniformity of thermal dissociation profile for each amplification product. Samples

without template or without reverse transcriptase were used as negative controls. Each RT-PCR reaction was performed in triplicate.

mTOR protein and mRNA quantification

Cells were lysed with RIPA buffer 1x (Cell Signaling) containing phosphatase inhibitors (PhosSTOP) and protease inhibitors (Complete Mini EDTA-free, Roche), for 10 minutes at 4°C and centrifuged at 14,000g for 10 min. Proteins were quantified in supernatants by Bradford assay (Biorad). Samples (15 µg protein/well) were loaded onto 7% acrylamide gels and SDS-PAGE migration was performed (90 min, 100 V). Proteins were transferred to PVDF membranes and further blotted with phosphorylated (D9C2) or total mTOR (7C10) Abs (Cell signaling). Proteins were revealed with ECL prime western blotting detection reagent (Amersham, GE Healthcare). In parallel, the expression of the mTOR mRNA was measured by semi-quantitative RT-PCR performed using the superscript III one-step RT-PCR system (Invitrogen, USA) and specific primers (forward: S1, ATGCTTGGAACCGGACCTGCCG ;   reverse: AS1, TACCAGAAAGGGCACCAGCCAAT) (Integrated DNA Technologies, USA) that could amplify both mTOR isoforms α (7.647Kb Kb) and β (2.118 Kb) (61) (Suppl. Figure 7A). However, the RT-PCR conditions were set for the optimal amplification of the short β mTOR isoform, as follows: reverse transcription (30 min at 55 °C), 40 cycles of PCR amplification (denaturation, 15 secs at 94 °C; annealing, 30 secs at 63 °C; elongation, 130 secs at 68 °C) and final elongation (15 min at 68 °C). mTOR expression was normalized relative to 28S rRNA. Total RNA was extracted using the RNeasy kit

(Qiagen) and used for RT-PCR amplification of mTOR (250 ng/test) and 28S rRNA (5 ng/test).

Nuclear NF-κB quantification

The NF-κB DNA-binding activity was quantified using an activity-based ELISA kit (Assay Designs & Stressgen, Ann Arbor, Mi, USA) according to the manufacturer's protocol, as described (20). Briefly, nuclear extracts were obtained using the BD transfactor extraction kit (Clonetech Laboratories). Nuclear protein content was quantified by Nanodrop (Thermo Scientific). The active form of NF-κB-p65 was quantified in nuclear extracts (1 μg protein/test). The assay used streptavidin-coated plates with bound NF-κB biotinylated-consensus sequence to capture only the active form of NF-κB. The captured NF-κB was then incubated with a specific NF-κB-p65 Abs further detected using an HRP conjugated Abs. The assay was developed with a chemiluminescent substrate and the signal was detected using a luminometer. Results were expressed as Light Units. The specificity of the binding was demonstrated by the use of a wild type and mutated NF-κB Competitor Duplex included in the kit.

ELISA quantification

HIV-p24 levels were quantified in cell culture supernatants using a homemade ELISA, as described (16, 19, 20, 36, 37, 42). Cytokine levels in cell culture supernatants were quantified by ELISA assays specific for TNF-α, CCL20 (R&D Systems), IL-17, IFN-γ and IL-2 (eBioscience) according to the manufacturers' protocols.

Viral outgrowth assay

This viral outgrowth assay (VOA) was designed to allow optimal HIV reservoir reactivation from small numbers of primary CD4$^+$ T-cells (36, 37). Briefly, memory CD4$^+$ T-cells (2x10^6 cells/ml/well) or FACS sorted memory CCR6$^+$/CCR6$^-$ T-cells (10^6 cells/ml/well) were cultured in 48-well plates in the presence of immobilized CD3 and soluble CD28 Abs (1 µg/ml) for 3 days. Cells were further cultured in the presence of IL-2 (5 ng/ml) up to day 12. Every 3 days, cells were split and media was refreshed. The VOA was performed in the presence/absence of ATRA (10 nM) and/or INK128 (50 nM). HIV-p24 levels were quantified by ELISA in cell culture supernatants, while intracellular HIV-p24 expression was quantified by flow cytometry at day 12 post-reactivation.

Statistics

Statistical analyses were performed using the GraphPad Prism 6. RM One-way ANOVA or ordinary ANOVA with Tukey's or Dunnetts's post-test were used for multiple comparisons. Two-tailed paired t-test was used for matched pairwise analyses. A P-value less than 0.05 was considered significant. (*, p-value<0.05; **, p-value<0.01; ***p-value<0.001; ****p-value<0.0001). Details are included in Figure legends.

Microarrays accession number

The entire microarray dataset and technical information requested by Minimum Information About a Microarray Experiment (MIAME) are available at the Gene Expression Omnibus database under accession number GSE93660.

Study approval

This study used biological samples (blood and sigmoid biopsies) from HIV-infected and uninfected participants and was conducted in compliance with the principles included in the Declaration of Helsinki. This study received approval from the Institutional Review Board of the McGill University Health Centre and the CHUM-Research Centre, Montreal, Quebec, Canada. All human participants provided written informed consent for their participation in the study and agreed with the publication of the scientific results.

Competing interests

The authors declare no financial and non-financial competing interests.

Authors' contributions

DP performed research, analyzed data, and wrote the manuscript. YZ and PM performed research and contributed to manuscript writing. JPG performed microarray data analysis and generated figures. AG performed research. AF contributed to research design and manuscript writing. NG and TJH provided protocols and reagents and contributed to research design. JPR provided access to clinical samples/information, set up clinical research protocols, and contributed to manuscript writing. PA designed research, analyzed data, and wrote the manuscript. All authors reviewed and accepted the manuscript.

Acknowledgements

References

1.	Deeks SG, Lewin SR, Ross AL, Ananworanich J, Benkirane M, Cannon P, Chomont N, Douek D, Lifson JD, Lo YR, et al. International AIDS Society global scientific strategy: towards an HIV cure 2016. *Nat Med.* 2016;22(8):839-50.

2.	Martin AR, and Siliciano RF. Progress Toward HIV Eradication: Case Reports, Current Efforts, and the Challenges Associated with Cure. *Annu Rev Med.* 2016;67(215-28.

3.	Lederman MM, Cannon PM, Currier JS, June CH, Kiem HP, Kuritzkes DR, Lewin SR, Margolis DM, McCune JM, Mellors JW, et al. A Cure for HIV Infection: "Not in My Lifetime" or "Just Around the Corner"? *Pathogens & immunity.* 2016;1(1):154-64.

4.	Mehandru S, Poles MA, Tenner-Racz K, Horowitz A, Hurley A, Hogan C, Boden D, Racz P, and Markowitz M. Primary HIV-1 infection is associated with preferential depletion of CD4+ T lymphocytes from effector sites in the gastrointestinal tract. *J Exp Med.* 2004;200(6):761-70.

5.	Brenchley JM, Schacker TW, Ruff LE, Price DA, Taylor JH, Beilman GJ, Nguyen PL, Khoruts A, Larson M, Haase AT, et al. CD4+ T cell depletion during all stages of HIV disease occurs predominantly in the gastrointestinal tract. *J Exp Med.* 2004;200(6):749-59.

6.	Brenchley JM, and Douek DC. Microbial translocation across the GI tract. *Annu Rev Immunol.* 2012;30(149-73.

7.	Schuetz A, Deleage C, Sereti I, Rerknimitr R, Phanuphak N, Phuang-Ngern Y, Estes JD, Sandler NG, Sukhumvittaya S, Marovich M, et al. Initiation of ART

during Early Acute HIV Infection Preserves Mucosal Th17 Function and Reverses HIV-Related Immune Activation. *PLoS Pathog.* 2014;10(12):e1004543.

8.   Wong JK, and Yukl SA. Tissue reservoirs of HIV. *Curr Opin HIV AIDS.* 2016;11(4):362-70.

9.   Liu R, Paxton WA, Choe S, Ceradini D, Martin SR, Horuk R, MacDonald ME, Stuhlmann H, Koup RA, and Landau NR. Homozygous defect in HIV-1 coreceptor accounts for resistance of some multiply-exposed individuals to HIV-1 infection. *Cell.* 1996;86(3):367-77.

10.   Wilkin TJ, and Gulick RM. CCR5 antagonism in HIV infection: current concepts and future opportunities. *Annu Rev Med.* 2012;63(81-93.

11.   Jessen H, Allen TM, and Streeck H. How a single patient influenced HIV research--15-year follow-up. *N Engl J Med.* 2014;370(7):682-3.

12.   Mora JR, and von Andrian UH. Retinoic acid: an educational "vitamin elixir" for gut-seeking T cells. *Immunity.* 2004;21(4):458-60.

13.   Arthos J, Cicala C, Martinelli E, Macleod K, Van Ryk D, Wei D, Xiao Z, Veenstra TD, Conrad TP, Lempicki RA, et al. HIV-1 envelope protein binds to and signals through integrin alpha4beta7, the gut mucosal homing receptor for peripheral T cells. *Nat Immunol.* 2008;9(3):301-9.

14.   Byrareddy SN, Arthos J, Cicala C, Villinger F, Ortiz KT, Little D, Sidell N, Kane MA, Yu J, Jones JW, et al. Sustained virologic control in SIV+ macaques after antiretroviral and alpha4beta7 antibody therapy. *Science.* 2016;354(6309):197-202.

15.   Gaffen SL, Jain R, Garg AV, and Cua DJ. The IL-23-IL-17 immune axis: from mechanisms to therapeutic testing. *Nat Rev Immunol.* 2014;14(9):585-600.

16.   Gosselin A, Monteiro P, Chomont N, Diaz-Griffero F, Said EA, Fonseca S, Wacleche V, El-Far M, Boulassel MR, Routy JP, et al. Peripheral blood CCR4+ CCR6+ and CXCR3+ CCR6+ CD4+ T cells are highly permissive to HIV-1 infection. *J Immunol.* 2010;184(3):1604-16.

17.   El Hed A, Khaitan A, Kozhaya L, Manel N, Daskalakis D, Borkowsky W, Valentine F, Littman DR, and Unutmaz D. Susceptibility of human Th17 cells to human immunodeficiency virus and their perturbation during infection. *J Infect Dis.* 2010;201(6):843-54.

18.   Alvarez Y, Tuen M, Shen G, Nawaz F, Arthos J, Wolff MJ, Poles MA, and Hioe CE. Preferential HIV Infection of CCR6+ Th17 Cells Is Associated with Higher Levels of Virus Receptor Expression and Lack of CCR5 Ligands. *J Virol.* 2013;87(19):10843-54.

19.   Bernier A, Cleret-Buhot A, Zhang Y, Goulet JP, Monteiro P, Gosselin A, Dafonseca S, Wacleche VS, Jenabian MA, Routy JP, et al. Transcriptional profiling reveals molecular signatures associated with HIV permissiveness in Th1Th17 cells and identifies Peroxisome Proliferator-Activated Receptor Gamma as an intrinsic negative regulator of viral replication. *Retrovirology.* 2013;10(1):160.

20.   Cleret-Buhot A, Zhang Y, Planas D, Goulet JP, Monteiro P, Gosselin A, Wacleche VS, Tremblay CL, Jenabian MA, Routy JP, et al. Identification of

novel HIV-1 dependency factors in primary CCR4CCR6Th17 cells via a genome-wide transcriptional approach. *Retrovirology.* 2015;12(1):102.

21.   Christensen-Quick A, Lafferty M, Sun L, Marchionni L, DeVico A, and Garzino-Demo A. Human Th17 Cells Lack HIV-Inhibitory RNases and Are Highly Permissive to Productive HIV Infection. *J Virol.* 2016;90(17):7833-47.

22.   Ruffin N, Brezar V, Ayinde D, Lefebvre C, Schulze Zur Wiesch J, van Lunzen J, Bockhorn M, Schwartz O, Hocini H, Lelievre JD, et al. Low SAMHD1 expression following T-cell activation and proliferation renders CD4+ T cells susceptible to HIV-1. *AIDS.* 2015;29(5):519-30.

23.   Touzot M, Grandclaudon M, Cappuccio A, Satoh T, Martinez-Cingolani C, Servant N, Manel N, and Soumelis V. Combinatorial flexibility of cytokine function during human T helper cell differentiation. *Nature communications.* 2014;5(3987.

24.   Stieh DJ, Matias E, Xu H, Fought AJ, Blanchard JL, Marx PA, Veazey RS, and Hope TJ. Th17 Cells Are Preferentially Infected Very Early after Vaginal Transmission of SIV in Macaques. *Cell Host Microbe.* 2016;19(4):529-40.

25.   McGary CS, Alvarez X, Harrington S, Cervasi B, Ryan ES, Iriele RI, Paganini S, Harper JL, Easley K, Silvestri G, et al. The loss of CCR6+ and CD161+ CD4+ T-cell homeostasis contributes to disease progression in SIV-infected rhesus macaques. *Mucosal Immunol.* 2017.

26.   Macal M, Sankaran S, Chun TW, Reay E, Flamm J, Prindiville TJ, and Dandekar S. Effective CD4+ T-cell restoration in gut-associated lymphoid tissue of HIV-

infected patients is associated with enhanced Th17 cells and polyfunctional HIV-specific T-cell responses. *Mucosal Immunol.* 2008;1(6):475-88.

27. McKinnon LR, and Kaul R. Quality and quantity: mucosal CD4+ T cells and HIV susceptibility. *Curr Opin HIV AIDS.* 2012;7(2):195-202.

28. Loiseau C, Requena M, Mavigner M, Cazabat M, Carrere N, Suc B, Barange K, Alric L, Marchou B, Massip P, et al. CCR6 regulatory T cells blunt the restoration of gut Th17 cells along the CCR6-CCL20 axis in treated HIV-1-infected individuals. *Mucosal Immunol.* 2016.

29. Kim CJ, Rousseau R, Huibner S, Kovacs C, Benko E, Shahabi K, Kandel G, Ostrowski M, and Kaul R. Impact of intensified antiretroviral therapy during early HIV infection on gut immunology and inflammatory blood biomarkers: a randomized controlled trial. *AIDS.* 2017.

30. Ortiz AM, Klase ZA, DiNapoli SR, Vujkovic-Cvijin I, Carmack K, Perkins MR, Calantone N, Vinton CL, Riddick NE, Gallagher J, et al. IL-21 and probiotic therapy improve Th17 frequencies, microbial translocation, and microbiome in ARV-treated, SIV-infected macaques. *Mucosal Immunol.* 2015.

31. Micci L, Ryan ES, Fromentin R, Bosinger SE, Harper JL, He T, Paganini S, Easley KA, Chahroudi A, Benne C, et al. Interleukin-21 combined with ART reduces inflammation and viral reservoir in SIV-infected macaques. *J Clin Invest.* 2015;125(12):4497-513.

32. d'Ettorre G, Rossi G, Scagnolari C, Andreotti M, Giustini N, Serafino S, Schietroma I, Scheri GC, Fard SN, Trinchieri V, et al. Probiotic supplementation promotes a reduction in T-cell activation, an increase in Th17 frequencies, and a

recovery of intestinal epithelium integrity and mitochondrial morphology in ART-treated HIV-1-positive patients. *Immun Inflamm Dis.* 2017.

33.   Ancuta P, Kamat A, Kunstman KJ, Kim EY, Autissier P, Wurcel A, Zaman T, Stone D, Mefford M, Morgello S, et al. Microbial translocation is associated with increased monocyte activation and dementia in AIDS patients. *PLoS ONE.* 2008;3(6):e2516.

34.   Sun H, Kim D, Li X, Kiselinova M, Ouyang Z, Vandekerckhove L, Shang H, Rosenberg ES, Yu XG, and Lichterfeld M. Th1/17 polarization of CD4 T cells supports HIV-1 DNA persistence during antiretroviral therapy. *J Virol.* 2015.

35.   Khoury G, Anderson JL, Fromentin R, Hartogenesis W, Smith MZ, Bacchetti P, Hecht FM, Chomont N, Cameron PU, Deeks SG, et al. Persistence of integrated HIV DNA in CXCR3 + CCR6 + memory CD4+ T cells in HIV-infected individuals on antiretroviral therapy. *AIDS.* 2016;30(10):1511-20.

36.   Wacleche VS, Goulet JP, Gosselin A, Monteiro P, Soudeyns H, Fromentin R, Jenabian MA, Vartanian S, Deeks SG, Chomont N, et al. New insights into the heterogeneity of Th17 subsets contributing to HIV-1 persistence during antiretroviral therapy. *Retrovirology.* 2016;13(1):59.

37.   Gosselin A, Wiche Salinas TR, Planas D, Wacleche VS, Zhang Y, Fromentin R, Chomont N, Cohen EA, Shacklett B, Mehraj V, et al. HIV persists in CCR6+CD4+ T cells from colon and blood during antiretroviral therapy. *AIDS.* 2017;31(1):35-48.

38. Wang C, Kang SG, Lee J, Sun Z, and Kim CH. The roles of CCR6 in migration of Th17 cells and regulation of effector T-cell balance in the gut. *Mucosal Immunol.* 2009;2(2):173-83.

39. Mavigner M, Cazabat M, Dubois M, L'Faqihi FE, Requena M, Pasquier C, Klopp P, Amar J, Alric L, Barange K, et al. Altered CD4+ T cell homing to the gut impairs mucosal immune reconstitution in treated HIV-infected individuals. *J Clin Invest.* 2012;122(1):62-9.

40. Wang C, Kang SG, HogenEsch H, Love PE, and Kim CH. Retinoic acid determines the precise tissue tropism of inflammatory Th17 cells in the intestine. *J Immunol.* 2010;184(10):5519-26.

41. Hall JA, Grainger JR, Spencer SP, and Belkaid Y. The role of retinoic acid in tolerance and immunity. *Immunity.* 2011;35(1):13-22.

42. Monteiro P, Gosselin A, Wacleche VS, El-Far M, Said EA, Kared H, Grandvaux N, Boulassel MR, Routy JP, and Ancuta P. Memory CCR6+CD4+ T cells are preferential targets for productive HIV type 1 infection regardless of their expression of integrin beta7. *J Immunol.* 2011;186(8):4618-30.

43. Parrish NF, Gao F, Li H, Giorgi EE, Barbian HJ, Parrish EH, Zajic L, Iyer SS, Decker JM, Kumar A, et al. Phenotypic properties of transmitted founder HIV-1. *Proc Natl Acad Sci U S A.* 2013;110(17):6626-33.

44. Ochsenbauer C, Edmonds TG, Ding H, Keele BF, Decker J, Salazar MG, Salazar-Gonzalez JF, Shattock R, Haynes BF, Shaw GM, et al. Generation of transmitted/founder HIV-1 infectious molecular clones and characterization of

their replication capacity in CD4 T lymphocytes and monocyte-derived macrophages. *J Virol.* 2012;86(5):2715-28.

45. He YW, Deftos ML, Ojala EW, and Bevan MJ. RORgamma t, a novel isoform of an orphan receptor, negatively regulates Fas ligand expression and IL-2 production in T cells. *Immunity.* 1998;9(6):797-806.

46. Goff SP. Knockdown screens to knockout HIV-1. *Cell.* 2008;135(3):417-20.

47. Kimura K, Zhou H, Orita T, Kobayashi S, Wada T, Nakamura Y, Nishida T, and Sonoda KH. Inhibition by all-trans retinoic acid of collagen degradation mediated by corneal fibroblasts. *Clin Exp Ophthalmol.* 2016;44(6):502-8.

48. Balmer JE, and Blomhoff R. Gene expression regulation by retinoic acid. *J Lipid Res.* 2002;43(11):1773-808.

49. Yu X, Rollins D, Ruhn KA, Stubblefield JJ, Green CB, Kashiwada M, Rothman PB, Takahashi JS, and Hooper LV. TH17 cell differentiation is regulated by the circadian clock. *Science.* 2013;342(6159):727-30.

50. Unutmaz D, Xiang W, Sunshine MJ, Campbell J, Butcher E, and Littman DR. The primate lentiviral receptor Bonzo/STRL33 is coordinately regulated with CCR5 and its expression pattern is conserved between human and mouse. *J Immunol.* 2000;165(6):3284-92.

51. Limou S, Coulonges C, Herbeck JT, van Manen D, An P, Le Clerc S, Delaneau O, Diop G, Taing L, Montes M, et al. Multiple-cohort genetic association study reveals CXCR6 as a new chemokine receptor involved in long-term nonprogression to AIDS. *J Infect Dis.* 2010;202(6):908-15.

52.   Richardson MW, Jadlowsky J, Didigu CA, Doms RW, and Riley JL. Kruppel-like factor 2 modulates CCR5 expression and susceptibility to HIV-1 infection. *J Immunol.* 2012;189(8):3815-21.

53.   Casazza JP, Brenchley JM, Hill BJ, Ayana R, Ambrozak D, Roederer M, Douek DC, Betts MR, and Koup RA. Autocrine production of beta-chemokines protects CMV-Specific CD4 T cells from HIV infection. *PLoS Pathog.* 2009;5(10):e1000646.

54.   Ramesh R, Kozhaya L, McKevitt K, Djuretic IM, Carlson TJ, Quintero MA, McCauley JL, Abreu MT, Unutmaz D, and Sundrud MS. Pro-inflammatory human Th17 cells selectively express P-glycoprotein and are refractory to glucocorticoids. *J Exp Med.* 2014;211(1):89-104.

55.   Klotz L, Burgdorf S, Dani I, Saijo K, Flossdorf J, Hucke S, Alferink J, Nowak N, Beyer M, Mayer G, et al. The nuclear receptor PPAR gamma selectively inhibits Th17 differentiation in a T cell-intrinsic fashion and suppresses CNS autoimmunity. *J Exp Med.* 2009;206(10):2079-89.

56.   Lahouassa H, Daddacha W, Hofmann H, Ayinde D, Logue EC, Dragin L, Bloch N, Maudet C, Bertrand M, Gramberg T, et al. SAMHD1 restricts the replication of human immunodeficiency virus type 1 by depleting the intracellular pool of deoxynucleoside triphosphates. *Nat Immunol.* 2012;13(3):223-8.

57.   Ryoo J, Choi J, Oh C, Kim S, Seo M, Kim SY, Seo D, Kim J, White TE, Brandariz-Nunez A, et al. The ribonuclease activity of SAMHD1 is required for HIV-1 restriction. *Nat Med.* 2014;20(8):936-41.

58.   Nagai S, Kurebayashi Y, and Koyasu S. Role of PI3K/Akt and mTOR complexes in Th17 cell differentiation. *Annals of the New York Academy of Sciences.* 2013;1280(30-4.

59.   Wan Q, Kozhaya L, ElHed A, Ramesh R, Carlson TJ, Djuretic IM, Sundrud MS, and Unutmaz D. Cytokine signals through PI-3 kinase pathway modulate Th17 cytokine production by CCR6+ human memory T cells. *J Exp Med.* 2011;208(9):1875-87.

60.   Kurebayashi Y, Nagai S, Ikejiri A, Ohtani M, Ichiyama K, Baba Y, Yamada T, Egami S, Hoshii T, Hirao A, et al. PI3K-Akt-mTORC1-S6K1/2 axis controls Th17 differentiation by regulating Gfi1 expression and nuclear translocation of RORgamma. *Cell reports.* 2012;1(4):360-73.

61.   Panasyuk G, Nemazanyy I, Zhyvoloup A, Filonenko V, Davies D, Robson M, Pedley RB, Waterfield M, and Gout I. mTORbeta splicing isoform promotes cell proliferation and tumorigenesis. *J Biol Chem.* 2009;284(45):30807-14.

62.   Heredia A, Le N, Gartenhaus RB, Sausville E, Medina-Moreno S, Zapata JC, Davis C, Gallo RC, and Redfield RR. Targeting of mTOR catalytic site inhibits multiple steps of the HIV-1 lifecycle and suppresses HIV-1 viremia in humanized mice. *Proc Natl Acad Sci U S A.* 2015;112(30):9412-7.

63.   Kelley CF, Kraft CS, de Man TJ, Duphare C, Lee HW, Yang J, Easley KA, Tharp GK, Mulligan MJ, Sullivan PS, et al. The rectal mucosa and condomless receptive anal intercourse in HIV-negative MSM: implications for HIV transmission and prevention. *Mucosal Immunol.* 2016.

64.   Bolduc JF, Ouellet M, Hany L, and Tremblay MJ. TLR2 ligation enhances HIV-1 replication in activated CCR6+CD4+ T cells by increasing virus entry and establishing a more permissive environment to infection. *J Virol.* 2016.

65.   Dillon SM, Lee EJ, Donovan AM, Guo K, Harper MS, Frank DN, McCarter MD, Santiago ML, and Wilson CC. Enhancement of HIV-1 infection and intestinal CD4+ T cell depletion ex vivo by gut microbes altered during chronic HIV-1 infection. *Retrovirology.* 2016;13(5.

66.   Liu Y, Olagnier D, and Lin R. Host and Viral Modulation of RIG-I-Mediated Antiviral Immunity. *Front Immunol.* 2016;7(662.

67.   Solis M, Nakhaei P, Jalalirad M, Lacoste J, Douville R, Arguello M, Zhao T, Laughrea M, Wainberg MA, and Hiscott J. RIG-I-mediated antiviral signaling is inhibited in HIV-1 infection by a protease-mediated sequestration of RIG-I. *J Virol.* 2011;85(3):1224-36.

68.   Li P, Kaiser P, Lampiris HW, Kim P, Yukl SA, Havlir DV, Greene WC, and Wong JK. Stimulating the RIG-I pathway to kill cells in the latent HIV reservoir following viral reactivation. *Nat Med.* 2016.

69.   Wang SF, Tsao CH, Lin YT, Hsu DK, Chiang ML, Lo CH, Chien FC, Chen P, Arthur Chen YM, Chen HY, et al. Galectin-3 promotes HIV-1 budding via association with Alix and Gag p6. *Glycobiology.* 2014;24(11):1022-35.

70.   Endsley MA, Somasunderam AD, Li G, Oezguen N, Thiviyanathan V, Murray JL, Rubin DH, Hodge TW, O'Brien WA, Lewis B, et al. Nuclear trafficking of the HIV-1 pre-integration complex depends on the ADAM10 intracellular domain. *Virology.* 2014;454-455(60-6.

71.   Konig R, Zhou Y, Elleder D, Diamond TL, Bonamy GM, Irelan JT, Chiang CY, Tu BP, De Jesus PD, Lilley CE, et al. Global analysis of host-pathogen interactions that regulate early-stage HIV-1 replication. *Cell.* 2008;135(1):49-60.

72.   Yeung ML, Houzet L, Yedavalli VS, and Jeang KT. A genome-wide short hairpin RNA screening of jurkat T-cells for human proteins contributing to productive HIV-1 replication. *J Biol Chem.* 2009;284(29):19463-73.

73.   Braunstein J, Autschbach F, Giese T, Lasitschka F, Heidtmann A, Sido B, Funke B, Reiser C, Schroder AJ, Nebl G, et al. Up-regulation of the phosphoinositide 3-kinase pathway in human lamina propria T lymphocytes. *Clin Exp Immunol.* 2008;151(3):496-504.

74.   Delgoffe GM, Pollizzi KN, Waickman AT, Heikamp E, Meyers DJ, Horton MR, Xiao B, Worley PF, and Powell JD. The kinase mTOR regulates the differentiation of helper T cells through the selective activation of signaling by mTORC1 and mTORC2. *Nat Immunol.* 2011;12(4):295-303.

75.   Maciolek JA, Pasternak JA, and Wilson HL. Metabolism of activated T lymphocytes. *Curr Opin Immunol.* 2014;27(60-74.

76.   Inoki K, Kim J, and Guan KL. AMPK and mTOR in cellular energy homeostasis and drug targets. *Annu Rev Pharmacol Toxicol.* 2012;52(381-400.

77.   Pollizzi KN, and Powell JD. Regulation of T cells by mTOR: the known knowns and the known unknowns. *Trends Immunol.* 2015;36(1):13-20.

78.   Nicoletti F, Fagone P, Meroni P, McCubrey J, and Bendtzen K. mTOR as a multifunctional therapeutic target in HIV infection. *Drug Discov Today.* 2011;16(15-16):715-21.

79. Le Sage V, Cinti A, Amorim R, and Mouland AJ. Adapting the Stress Response: Viral Subversion of the mTOR Signaling Pathway. *Viruses.* 2016;8(6).

80. Robitaille AM, Christen S, Shimobayashi M, Cornu M, Fava LL, Moes S, Prescianotto-Baschong C, Sauer U, Jenoe P, and Hall MN. Quantitative phosphoproteomics reveal mTORC1 activates de novo pyrimidine synthesis. *Science.* 2013;339(6125):1320-3.

81. Chen W, Zhang L, Zhang K, Zhou B, Kuo ML, Hu S, Chen L, Tang M, Chen YR, Yang L, et al. Reciprocal regulation of autophagy and dNTP pools in human cancer cells. *Autophagy.* 2014;10(7):1272-84.

82. Matsuzawa Y, Oshima S, Takahara M, Maeyashiki C, Nemoto Y, Kobayashi M, Nibe Y, Nozaki K, Nagaishi T, Okamoto R, et al. TNFAIP3 promotes survival of CD4 T cells by restricting MTOR and promoting autophagy. *Autophagy.* 2015;11(7):1052-62.

83. Borel S, Espert L, and Biard-Piechaczyk M. Macroautophagy Regulation during HIV-1 Infection of CD4+ T Cells and Macrophages. *Front Immunol.* 2012;3(97.

84. Sagnier S, Daussy CF, Borel S, Robert-Hebmann V, Faure M, Blanchet FP, Beaumelle B, Biard-Piechaczyk M, and Espert L. Autophagy restricts HIV-1 infection by selectively degrading Tat in CD4+ T lymphocytes. *J Virol.* 2015;89(1):615-25.

85. McGuire DJ, Rowse AL, Li H, Peng BJ, Sestero CM, Cashman KS, De Sarno P, and Raman C. CD5 enhances Th17-cell differentiation by regulating IFN-gamma response and RORgammat localization. *Eur J Immunol.* 2014;44(4):1137-42.

86.	Besnard E, Hakre S, Kampmann M, Lim HW, Hosmane NN, Martin A, Bassik MC, Verschueren E, Battivelli E, Chan J, et al. The mTOR Complex Controls HIV Latency. *Cell Host Microbe.* 2016;20(6):785-97.

87.	Martin AR, Pollack RA, Capoferri A, Ambinder RF, Durand CM, and Siliciano RF. Rapamycin-mediated mTOR inhibition uncouples HIV-1 latency reversal from cytokine-associated toxicity. *J Clin Invest.* 2017.

88.	Boulassel MR, Spurll G, Rouleau D, Tremblay C, Edwardes M, Sekaly RP, Lalonde R, and Routy JP. Changes in immunological and virological parameters in HIV-1 infected subjects following leukapheresis. *J Clin Apher.* 2003;18(2):55-60.

89.	Shacklett BL, Yang O, Hausner MA, Elliott J, Hultin L, Price C, Fuerst M, Matud J, Hultin P, Cox C, et al. Optimization of methods to assess human mucosal T-cell responses to HIV infection. *J Immunol Methods.* 2003;279(1-2):17-31.

90.	Hayes TL, Asmuth DM, Critchfield JW, Knight TH, McLaughlin BE, Yotter T, McConnell DH, Garcia JC, Pollard RB, and Shacklett BL. Impact of highly active antiretroviral therapy initiation on CD4(+) T-cell repopulation in duodenal and rectal mucosa. *AIDS.* 2013;27(6):867-77.

91.	Roederer M. Compensation in flow cytometry. *Current protocols in cytometry / editorial board, J Paul Robinson, managing editor [et al].* 2002;Chapter 1(Unit 1 14.

92.	Ancuta P, Kunstman KJ, Autissier P, Zaman T, Stone D, Wolinsky SM, and Gabuzda D. CD16+ monocytes exposed to HIV promote highly efficient viral

replication upon differentiation into macrophages and interaction with T cells. *Virology.* 2006;344(2):267-76. .

93. Chomont N, El-Far M, Ancuta P, Trautmann L, Procopio FA, Yassine-Diab B, Boucher G, Boulassel MR, Ghattas G, Brenchley JM, et al. HIV reservoir size and persistence are driven by T cell survival and homeostatic proliferation. *Nat Med.* 2009;15(8):893-900.

94. Bakri Y, Schiffer C, Zennou V, Charneau P, Kahn E, Benjouad A, Gluckman JC, and Canque B. The maturation of dendritic cells results in postintegration inhibition of HIV-1 replication. *J Immunol.* 2001;166(6):3780-8.
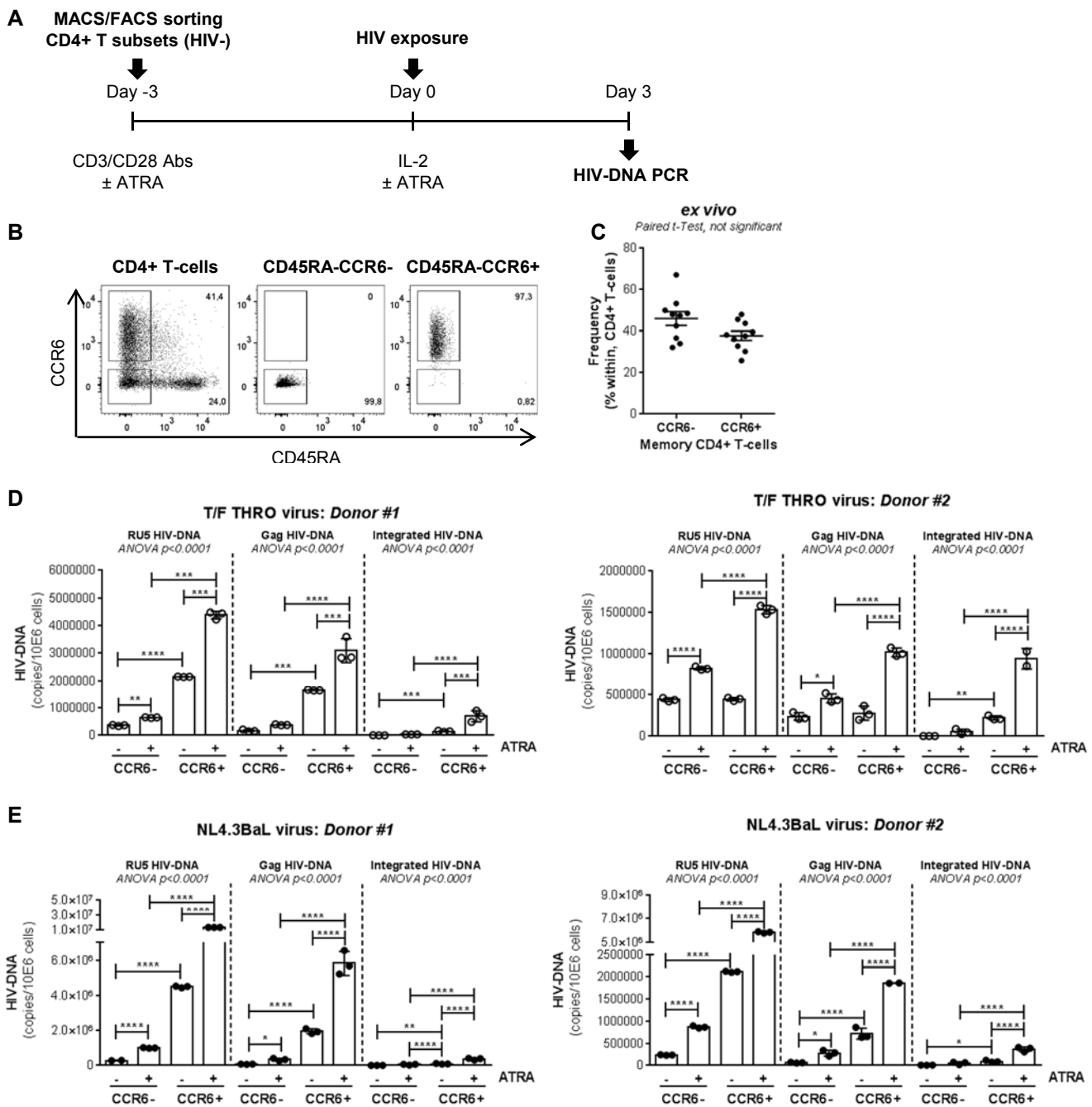
Figure 1: Replication advantage of transmitted founder HIV in CCR6+ *versus* CCR6- T-cells upon exposure to ATRA. Memory CCR6+ and CCR6- T-cells were isolated by MACS (magnetic-activated cell sorting) and FACS from the PBMCs (peripheral blood mononuclear cells) of HIV-uninfected individuals and tested for their ability to replicate HIV *in vitro*. Shown is **(A)** the experimental flow chart, **(B)** the expression of CCR6 and CD45RA on total CD4+ T-cells isolated using magnetic beads and on memory (CD45RA-) CCR6+ and CCR6- T-cells isolated by FACS, and **(C)** the frequency of CCR6- and CCR6+ T-cells within memory CD4+ T-cells in n=10 donors. Paired t-Test p-values are indicated on the graphs **(D-E)**. Sorted cells were stimulated *via* CD3/CD28 in presence/absence of ATRA (*all-trans retinoic acid*) (10 nM) for 4 days and exposed to **(D)** transmitted founder (T/F) THRO HIV or (E) laboratory-adapted NL4.3BaL HIV (25 ng HIV-p24/10⁶ cells). Early (RU5 primers) and late (Gag primers) HIV-DNA reverse transcripts, as well as integrated HIV-DNA levels (Alu/HIV-LTR primers) were quantified by nested real-time PCR in matched subsets isolated from n=2 different donors at day 3 post-infection (mean±SD of triplicate wells). **(D-E)** One-way ANOVA p-values with the significance of the Tukey's multiple comparisons test are indicated on the figures. Each symbol represents one triplicate value.
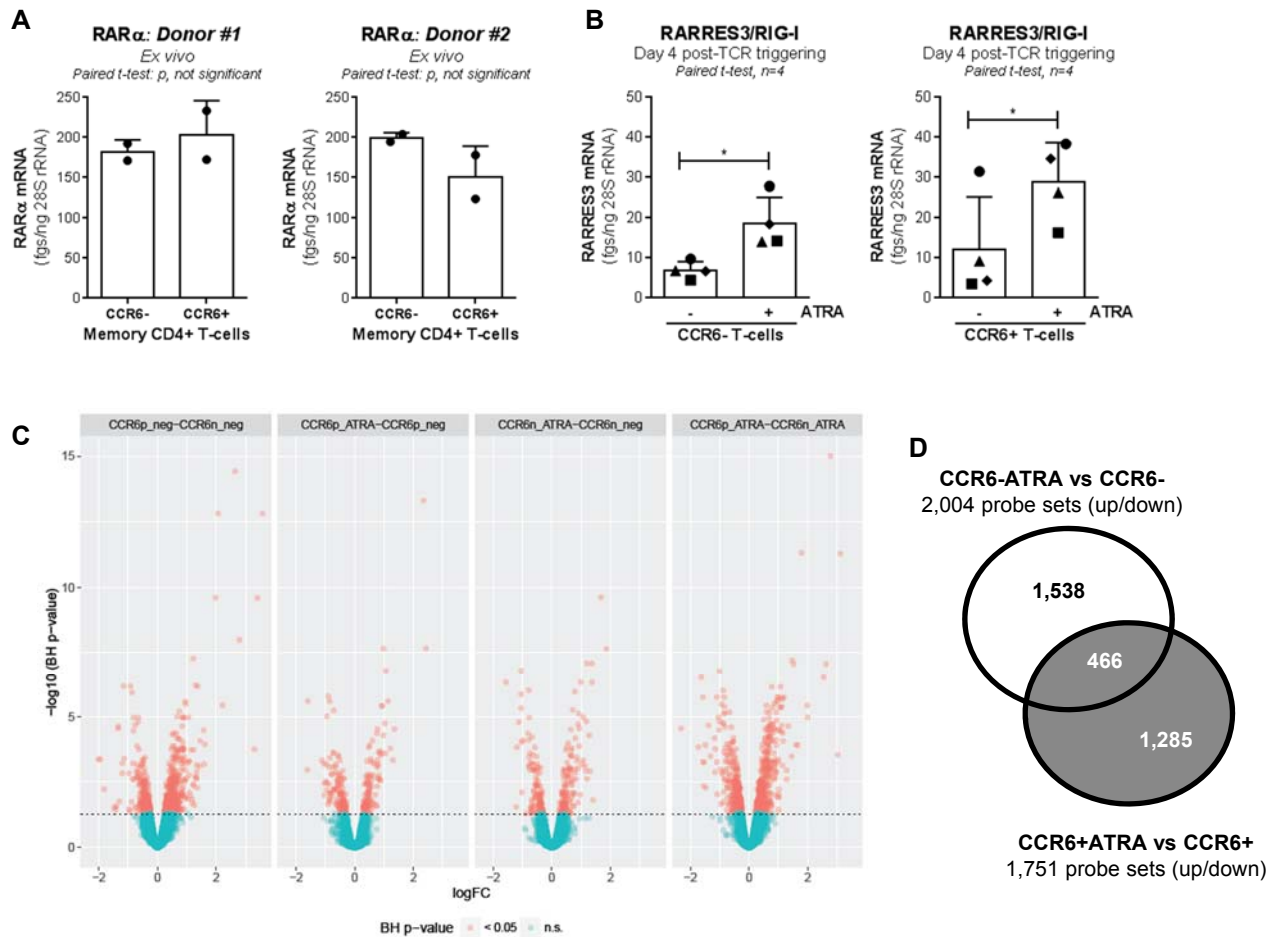
Figure 2: ATRA differentially modulates gene expression in CCR6⁻ and CCR6⁺ T-cells. Memory CCR6⁺/CCR6⁻ T-cells were sorted and stimulated as described in Figure 1. Shown is the SYBR green real-time RT-PCR quantification of RARα (retinoic acid receptor α) mRNA *ex vivo* (A; n=2, mean±SD) and RIG-I/RARRES3 (retinoic acid induced gene I) mRNA upon CD3/CD28 triggering in the presence/absence of ATRA (B; n=4, mean±SEM). **(A-B)** Paired t-Test p-values are indicated on the graphs. Each symbol represents **(A)** one duplicate value or **(B)** one different donor. **(C-E)** Total RNA from matched T-cell subsets of n=6 different HIV-uninfected donors was used for genome-wide transcriptional profiling. One-way ANOVA analysis identified differentially expressed genes based on p-values or adjusted p-values (<0.05) and/or fold-change (FC, cut-off 1.3). **(C)** Shown are volcano plots for all probes in each linear model with the log2 FC on the x axis and the negative logarithm of the adjusted p-values for false discovery rate (FDR) on the y axis. The red/green color code is based on the 5% FDR threshold. **(D)** The Venn diagram depicts the number of probe-sets modulated by ATRA uniquely in CCR6⁺ (grey) and CCR6⁻ T-cells (white) (p-values<0.05), as well as 466 probe sets commonly modulated.
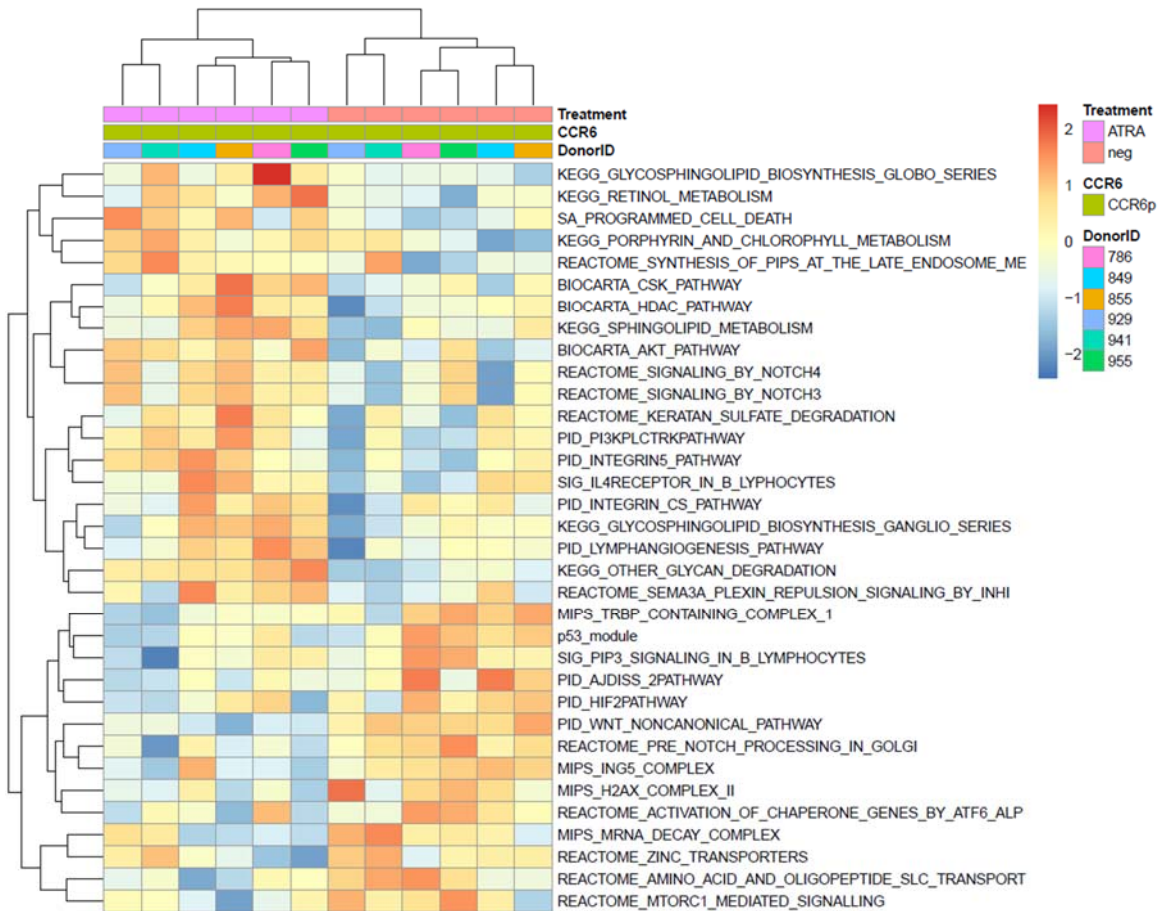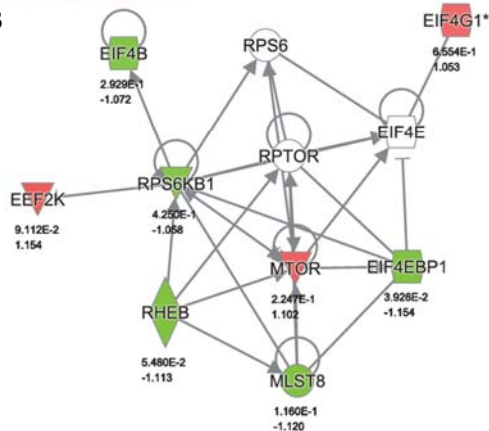
Figure 3: Canonical pathways modulated by ATRA in CCR6+ T-cells. Memory CCR6+/CCR6- T-cells were sorted and stimulated as described in Figure 1. Total RNA from matched T-cell subsets of n=6 different HIV-uninfected donors was used for genome-wide transcriptional profiling as described in Figure 2. One-way ANOVA analysis identified differentially expressed genes based on p-values or adjusted p-values (<0.05) and/or fold-change (FC, cut-off 1.3). The heat map depicts top 34 pathways up (red) and down (blue) modulated by ATRA in CCR6+ T-cells, identified using gene-set variation analysis (GSVA; p-value<0.01;enrichment z-score).

A
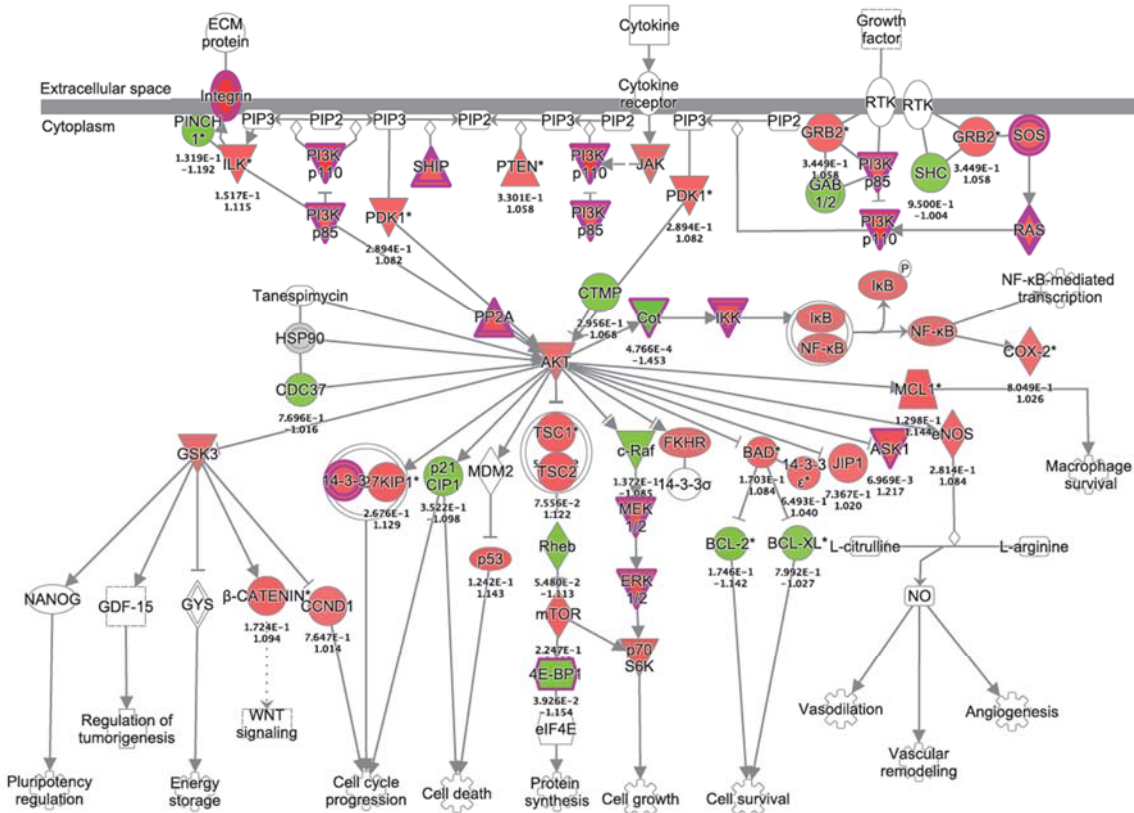
B

Figure 4: Components of the AKT/PI3K pathways modulated by ATRA in CCR6+ T-cells. Memory CCR6+/CCR6- T-cells were sorted and stimulated as described in Figure 1. Total RNA from matched T-cell subsets of n=6 different HIV-uninfected donors was used for genome-wide transcriptional profiling as described in Figure 2. One-way ANOVA analysis identified differentially expressed genes based on p-values or adjusted p-values (<0.05) and/or fold-change (FC, cut-off 1.3). Shown are *(A)* combined BIOCARTA_AKT_PATHWAY and PID_PI3K_PLC_TRK_PATHWAY Canonical pathways significantly modulated by ATRA in CCR6+ T-cells, identified using Ingenuity Pathway Analysis®; and **(B)** Gene expression network generated using individual genes representing REACTOME_MTORC1_MEDIATED_SIGNALING, significantly modulated by ATRA in CCR6+ T-cells identified through GSVA. The color code is based on expression FC (red and green for up-regulated and down-regulated transcripts, respectively). Nodes representing individual genes are annotated with their corresponding p-values and FC.

Planas *et al.*, Figure 4
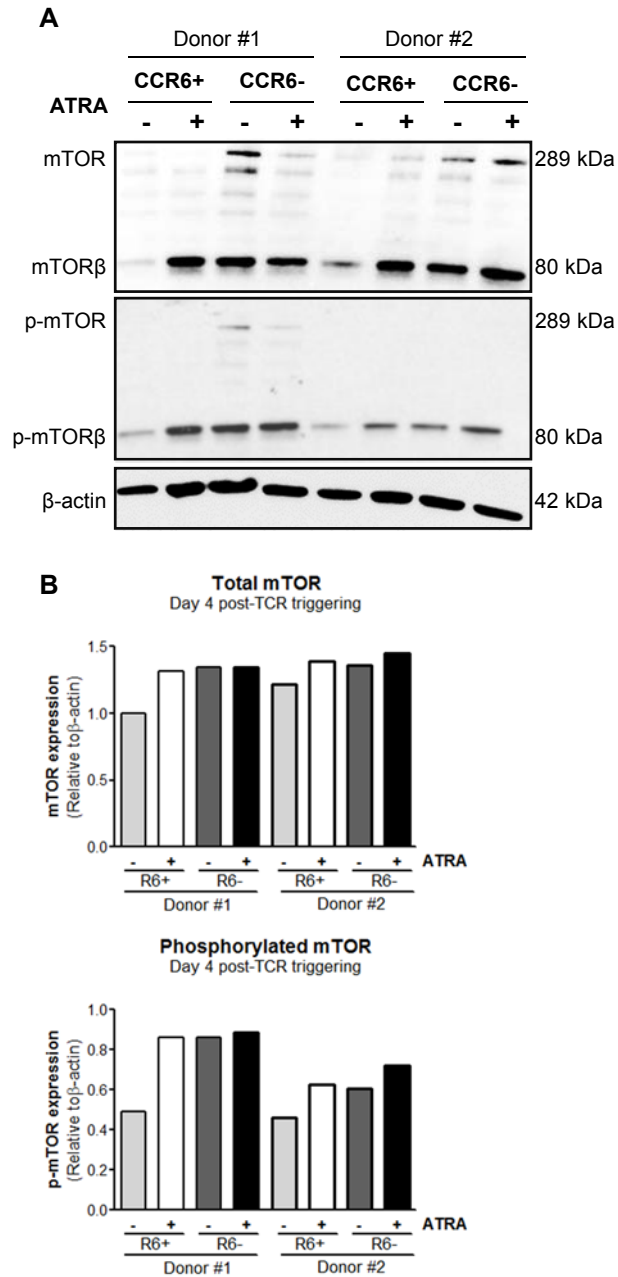
Figure 5: ATRA induces mTOR expression and phosphorylation selectively in CCR6+ T-cells. Memory CCR6+ and CCR6- T-cell subsets were sorted and stimulated as described in Figure 1. **(A)** Cell lysates were used to visualize total and phosphorylated mTOR expression by Western Blotting. **(B)** Levels of total and phosphorylated mTOR expression were quantified by densitometry and normalized relative to β-actin levels. Of note, the molecular weight of the predominant mTOR band was 80 kDa, corresponding to the β isoform of mTOR (1). Shown are results obtained with cells from two different donors.
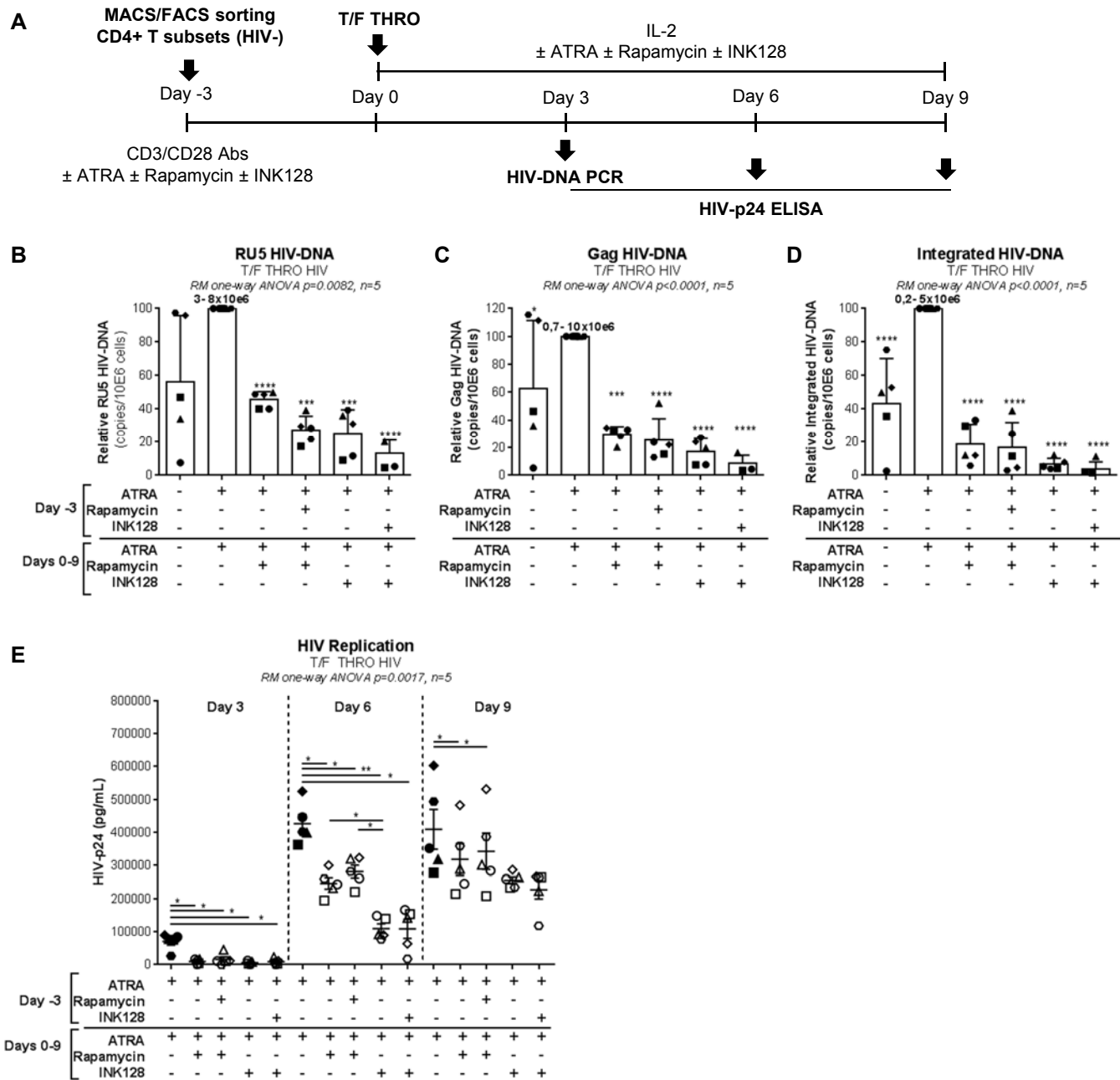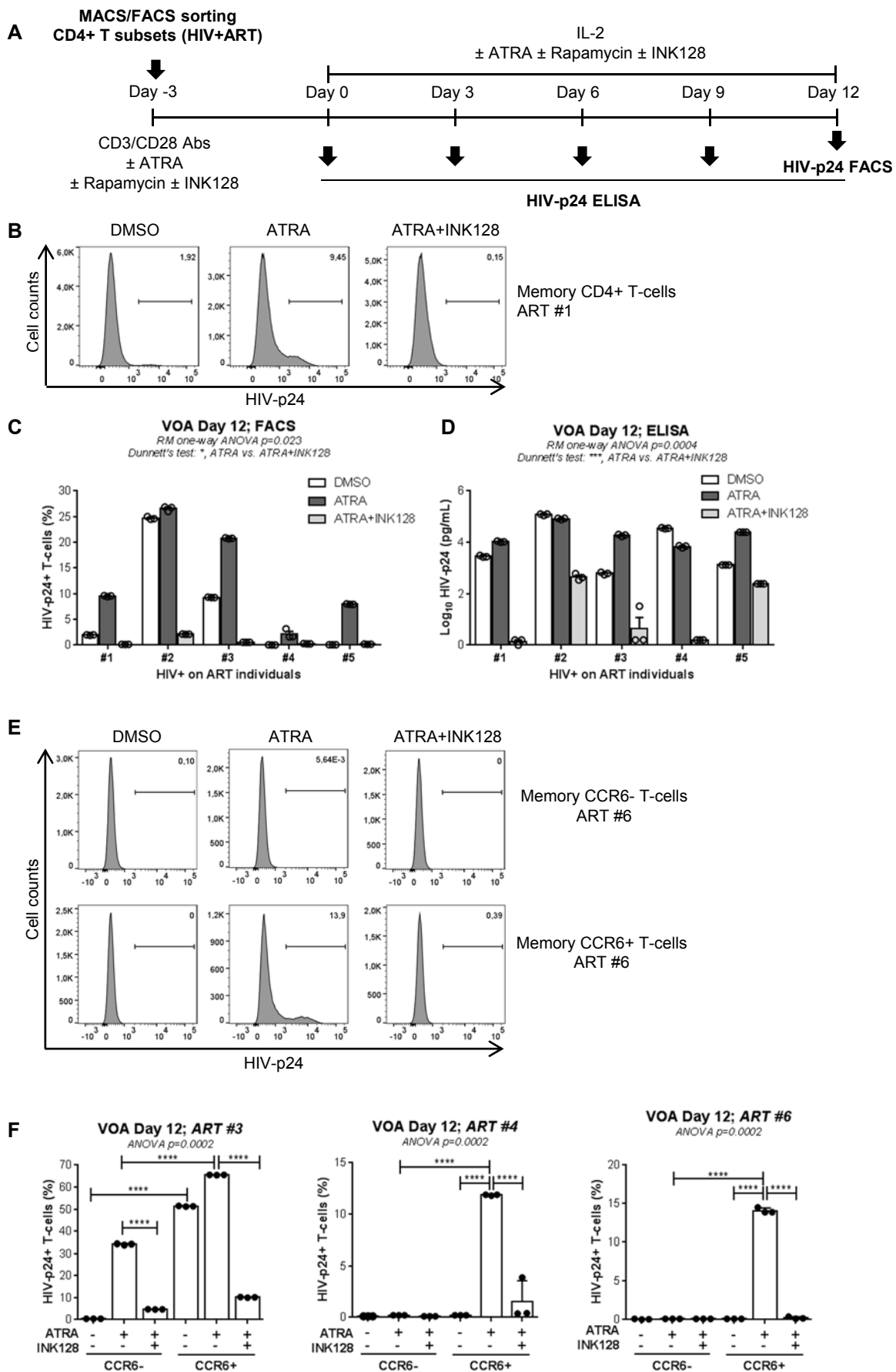
Figure 6: mTOR inhibitors counteract the effect of ATRA on HIV permissiveness in memory CD4+ T-cells. The ability of mTOR inhibitors to counteract the effects of ATRA on HIV replication was tested in total memory CD4^{+} T-cells **(A)**. Briefly, total memory CD4^{+} T-cells were stimulated *via* CD3/CD28 in presence/absence of ATRA and/or rapamycin (10 nM) or INK128 (50 nM) for 4 days. Then, cells were exposed to replication competent T/F HIV THRO (25 ng HIV-p24/10^6 cells). Further, cells were cultured for 9 additional days in presence/absence of ATRA and/or rapamycin or INK128. Shown are the relative RU5, Gag, and integrated HIV-DNA levels quantified by real-time nested PCR at day 3 post-infection (with the range of absolute HIV-DNA copies/10^6 cells in ATRA-treated cells, considered 100%, being indicated on the figures) **(B-D)** and HIV-p24 levels quantified by ELISA in cell culture supernatants at days, 3, 6 and 9 post-infection **(E)** (n=5, mean±SEM) . The RM one-way ANOVA p-values **(B-E)**, with the significance of the Dunnetts's (relative to cells stimulated *via* the TCR in the presence of ATRA) **(B-C-D)** or Tukey's **(E)** multiple comparisons test are indicated on the figures. Each symbol represents one different donor.
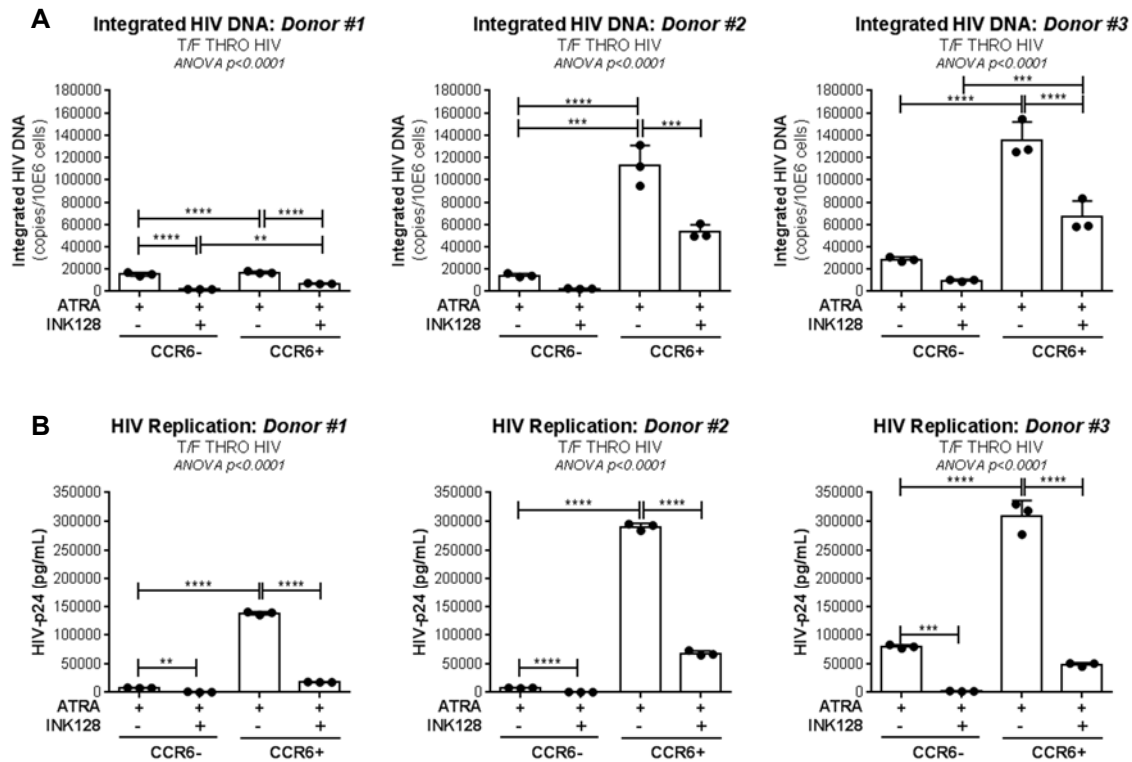
Figure 7: mTOR inhibitors counteract the effect of ATRA on HIV permissiveness in sorted CCR6+ and CCR6- T-cells. Memory CCR6+ and CCR6- T-cells were sorted as depicted in Figure 1 and stimulated *via* CD3/CD28 in presence of ATRA or ATRA and INK128 (50 nM) for 4 days. Then, cells were exposed to replication competent T/F HIV THRO (25 ng HIV-p24/10^6 cells). Further, cells were cultured for 9 additional days in presence of ATRA or ATRA and INK128. **(A-B)** Shown are absolute levels of integrated HIV-DNA at day 3 post-infection **(A)** and HIV-p24 levels in cell culture supernatants at day 6 post-infection **(B)** (n=3, mean±SD of triplicate wells), Ordinary one-way ANOVA with the significance of the Tukey's multiple comparisons test are indicated on the figures. Each symbol represents one experimental triplicate value in individual donors.
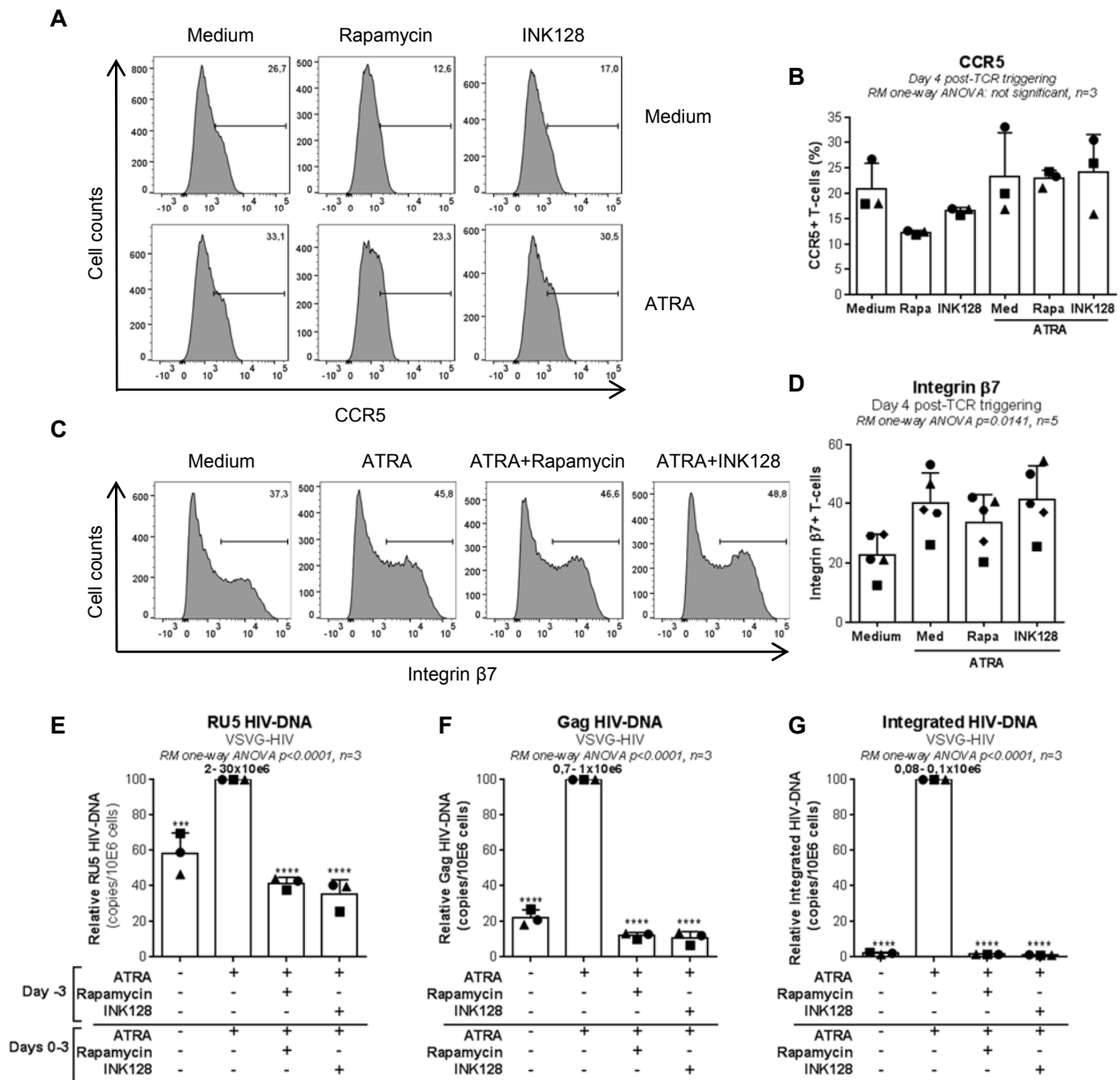
Figure 8: mTOR inhibitors limit HIV replication at post-entry levels in ATRA-treated CD4+ T-cells. (A-D) Memory CD4+ T-cells were first analyzed for the surface expression of CCR5 and integrin β7 at day 4 post-TCR triggering in the presence/absence of ATRA (10 nM), rapamycin (10nM), and/or INK128 (50nM). Shown are levels of CCR5 **(A)** and integrin β7 **(C)** expression in one representative donor and statistical analysis of CCR5 (**B**; n=3) and integrin β7 (**D**; n=5) expression in different donors (mean±SEM). **(E-G)** Then, stimulated cells were exposed to VSV-G-pseudotyped HIV (25 ng HIV-p24/10^6 cells) (single round infection) and cultured in presence/absence of ATRA and/or rapamycin or INK128 for 3 additional days. Levels of RU5 **(E)**, Gag **(F)** and integrated HIV-DNA **(G)** were quantified by nested real-time PCR in cells harvested at day 3 post-infection. **(E-G)** Shown are relative HIV-DNA levels (mean±SEM; n=3); the range of absolute HIV-DNA copies/10^6 cells in ATRA-treated CCR6+ T-cells (considered 100%) is indicated on the figure. The RM one-way ANOVA p-values with the significance of the Tukey's **(B-D)** or Dunnetts's (relative to cells stimulated *via* the TCR the presence of ATRA) **(E, F, G)** multiple comparisons tests are indicated on the graphs. Each symbol represents one different donor.

A

IL-2
± ATRA ± Rapamycin ± INK128

Day -3   Day 0   Day 3   Day 6   Day 9   Day 12

CD3/CD28 Abs
± ATRA
± Rapamycin ± INK128

HIV-p24 FACS

HIV-p24 ELISA

B

Memory CD4+ T-cells
ART #1

C

VOA Day 12; FACS
RM one-way ANOVA p=0.023
*Dunnett's test: *, ATRA vs. ATRA+INK128*

D

VOA Day 12; ELISA
RM one-way ANOVA p=0.0004
*Dunnett's test: ***, ATRA vs. ATRA+INK128*

E

Memory CCR6- T-cells
ART #6

Memory CCR6+ T-cells
ART #6

F

VOA Day 12; *ART #3*
ANOVA p=0.0002

VOA Day 12; *ART #4*
ANOVA p=0.0002

VOA Day 12; *ART #6*
*ANOVA p=0.0002*

Planas *et al.*, Figure 9

Figure 9: Drug-mediated mTOR blockade counteracts the enhancing effects of ATRA on HIV reactivation in a viral outgrowth assay. HIV reactivation was measured in a viral outgrowth assay (VOA), as summarized in the flowchart **(A)**. Briefly, total memory CD4$^+$ T-cells **(B-D**; n=5) and FACS-sorted memory CCR6+ and CCR6- T-cells (**E-F**; n=3) were isolated from PBMCs of HIV+ART individuals (Table S5; ART#1-6). Cells were activated *via* CD3/CD28 and cultured in presence/absence of ATRA (10 nM) and/or INK128 (50 nM). Shown is intracellular HIV-p24 expression in total memory CD4+ T-cells **(B-C)** and sorted memory CCR6+ and CCR6- T-cells **(E-F)** quantified by FACS, as well as HIV-p24 levels quantified by ELISA in cell culture supernatants of total memory CD4+ T-cells **(D)** harvested at day 12 post-activation. Results are depicted in individual donors. Each point represents one experimental triplicate (mean±SD of triplicate wells). The RM one-way ANOVA p-values with the significance of the Dunnetts's multiple comparisons test (relative to cells stimulated *via* the TCR the presence of ATRA) **(C-D)** and the ordinary one-way ANOVA with the significance of the Tukey's multiple comparisons test **(F)** are indicated in the figures.
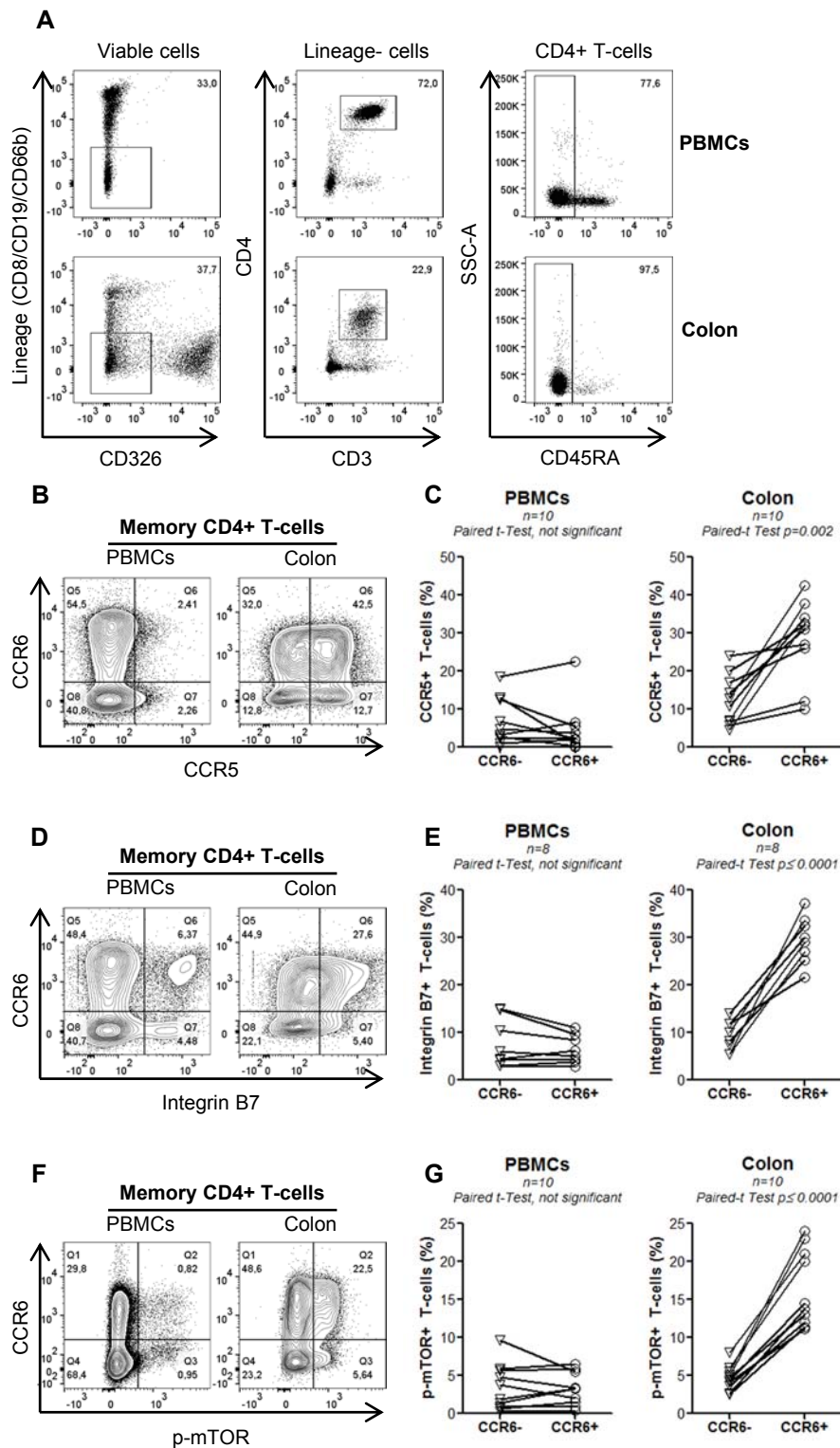
Figure 10: Memory CCR6+CD4+ T-cells infiltrating the colon of HIV+ART individuals express high levels of CCR5, integrin β7, and phosphorylated mTOR. Matched blood and sigmoid biopsies were collected from HIV-infected individuals with undetectable plasma viral load (<40 HIV-RNA copies/ml) under ART (Table S5; COL#1-10). Cells were extracted and stained with a cocktail of specific Abs. Shown is the gating strategy for the flow cytometry identification of CD3+CD4+CD45RA− T-cells **(A)**, as well as the surface expression of CCR5 **(B-C)** and integrin β7 **(D-E)** and the intracellular expression of phosphorylated mTOR **(F-G)** on CCR6+ and CCR6− subsets from sigmoid biopsies *versus* PBMC in one representative donor (B, D, and F) and statistical analysis in all donors **(C, E, and G)**. Paired t-Test values are indicated on the graphs.
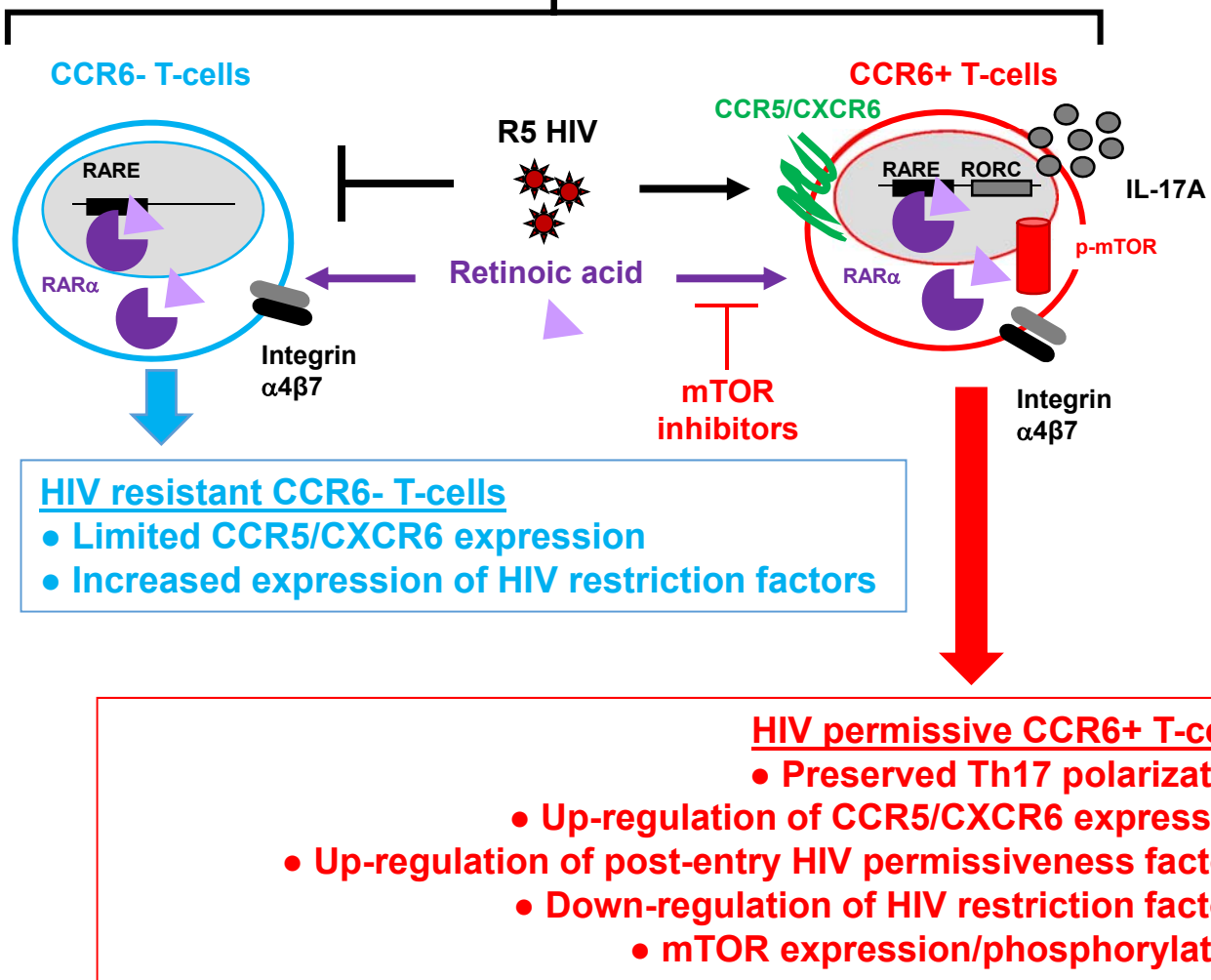
Figure 11: Mechanisms contributing to HIV replication in gut-homing CCR6+ T-cells. In this manuscript, we provide evidence that CCR6 is a marker for memory CD4+ T-cells programmed to become HIV targets, especially in the intestinal environment rich in retinoic acid, due to their expression of a unique Th17-polarized transcriptional program and a mTOR-governed metabolic state. We propose the use of mTOR inhibitors together with ART to protect gut-homing Th17 cells from HIV infection/persistence.